Available online at www.sciencedirect.com

ScienceDirect

Geochimica et Cosmochimica Acta 193 (2016) 14–35

Geochimica et Cosmochimica Acta

www.elsevier.com/locate/gca

Neodymium isotopes in authigenic phases, bottom waters and detrital sediments in the Gulf of Alaska and their implications for paleo-circulation reconstruction

Jianghui Du *, Brian A. Haley, Alan C. Mix

College of Earth, Ocean, and Atmospheric Sciences, Oregon State University, 104 CEOAS Admin. Bldg., Corvallis, OR 97331-5503, United States

Received 26 January 2016; accepted in revised form 4 August 2016; available online 10 August 2016

Abstract

The isotopic composition of neodymium (ε_{Nd}) extracted from sedimentary Fe–Mn oxyhydroxide offers potential for reconstructing paleo-circulation, but its application depends on extraction methodology and the mechanisms that relate authigenic ε_{Nd} to bottom water. Here we test methods to extract authigenic ε_{Nd} from Gulf of Alaska (GOA) sediments and assess sources of leachate Nd, including potential contamination from trace dispersed volcanic ash. We show that one dominant phase is extracted via leaching of core-top sediments. Major and trace element geochemistry demonstrate that this phase is authigenic Fe–Mn oxyhydroxide. Contamination of leachate (authigenic) Nd from detrital sources is insignificant (<1%); our empirical results are consistent with established kinetic mineral dissolution rates and theory. Contamination of extracted ε_{Nd} from leaching of volcanic ash is below analytical uncertainty. However, the ε_{Nd} of core-top leachates in the GOA is consistently more radiogenic than bottom water. We infer that authigenic phases record pore water ε_{Nd}, and the relationships of ε_{Nd} among bottom waters, pore waters, authigenic phases and detrital sediments are primarily governed by the exposure time of bottom water to sea-floor sediments, rate of exchange across the sediment-water interface and the reactivity and composition of detrital sediments. We show that this conceptual model is applicable on the Pacific basin scale and provide a new framework to understand the role of authigenic phases in both modern and paleo-applications, including the use of authigenic ε_{Nd} as a paleo-circulation tracer.

Key words: Authigenic phases; Pore water; Detrital sediments; Neodymium isotope composition; Early diagenesis; Sediment-water interaction; Gulf of Alaska; North Pacific; Paleo-circulation

1. INTRODUCTION

The isotopic composition of neodymium (ε_{Nd}) of seawater has attracted wide attention in the paleoceanography community as it is considered to be free from complications such as biological fractionation and gas exchange, and therefore can hypothetically be used as a quasi-conservative circulation tracer in the ocean interior (Frank, 2002; Goldstein and Hemming, 2003). This application of ε_{Nd} builds on an assumption that its heterogeneity in the ocean is inherited from the surrounding continents and persists in water masses. This framework suggests an oceanic residence time of Nd shorter than the ~1000 yr time scale of global overturning circulation (Goldstein and Hemming, 2003; Tachikawa et al., 2003).

Current debates on the oceanic cycle of Nd are centered on two related issues: the sources of marine Nd and the contrasting behaviors of Nd concentration and ε_{Nd} (commonly referred to as the Nd paradox) (Tachikawa et al.,

* Corresponding author.
E-mail address: dujia@oregonstate.edu (J. Du).

http://dx.doi.org/10.1016/j.gca.2016.08.005
0016-7037/

2003; Arsouze et al., 2009; Jeandel and Oelkers, 2015). Recent assessments of the oceanic Nd budget suggest atmospheric and dissolved riverine inputs are only minor sources, and to close the budget some "missing" sources are required (Tachikawa et al., 2003; Jones et al., 2008; Arsouze et al., 2009; Rempfer et al., 2011). One study suggested potential contribution from submarine groundwater discharge (Johannesson and Burdige, 2007). A recent study of riverine sources showed that although the dissolved Nd flux is small, the amount of Nd released from suspended sediments in river estuaries could be globally significant (Rousseau et al., 2015). Lacan and Jeandel (2005) proposed the "boundary exchange" concept to reconcile the elemental and isotopic budgets of Nd, but this remains an umbrella term that could refer to a suite of unidentified processes. While the original proposition emphasized "exchange", subsequent investigations were more suggestive of a "boundary source" generally limited to the margins (Arsouze et al., 2009; Rempfer et al., 2011; Wilson et al., 2012). Another mechanism proposed to resolve the Nd paradox, reversible scavenging (Siddall et al., 2008), is based on well-established ideas (Bacon and Anderson, 1982; Bertram and Elderfield, 1993), but awaits validation through better sampling of particulates in the ocean (Jeandel and Oelkers, 2015). A different line of work focuses on the influence of pore water and early diagenesis on the marine Nd cycle (Elderfield and Sholkovitz, 1987; Sholkovitz and Elderfield, 1988; Sholkovitz et al., 1989, 1992; Haley et al., 2004; Schacht et al., 2010; Abbott et al., 2015a). The effect of benthic flux on bottom water ε_{Nd} distribution was recently quantified in the Northeast Pacific with pore water ε_{Nd} measurements (Abbott et al., 2015b, 2016). One key discovery is that the heterogeneity of sediments in terms of reactivity and isotope composition does play a critical role in the diagenetic and oceanic cycles of Nd (Wilson et al., 2013; Abbott et al., 2015b, 2016). These works further find, perhaps counterintuitively, that the mobilization of Nd and other Rare Earth Elements (REEs) during early diagenesis is more favored at greater water depths that are typical of open ocean conditions, and its relationship to the redox cycles of Fe and Mn is complicated (Haley and Klinkhammer, 2003; Haley et al., 2004; Schacht et al., 2010; Abbott et al., 2015a,b, 2016). Indeed, while the data are yet spatially limited, there is no mechanistic reason to suggest that the benthic flux is limited to the margins, as might be inferred from the boundary exchange paradigm, and existing data are also not consistent with a surficial sink linked to the presence of Fe–Mn oxides in oxic sediments (Haley and Klinkhammer, 2003; Haley et al., 2004; Abbott et al., 2016). Despite such significant advances, sediment-water interaction remains one of the least understood aspects of the oceanic cycle of Nd.

In addition to uncertainties regarding the modern oceanic processes that control Nd concentrations and isotopic compositions in authigenic phases, the application of ε_{Nd} in paleoceanography relies on careful extraction of authigenic ε_{Nd} without contamination. Planktonic foraminifera and fish debris are viewed favorably as authigenic archives because removal of potential contaminating phases is easier than from bulk sediments (Tachikawa et al., 2013, 2014). These archives present practical challenges, however, because they are not present in all areas of the ocean, and their extraction is labor intensive. Retrieving ε_{Nd} signals from authigenic Fe–Mn oxyhydroxide coatings by leaching of bulk sediment offers an advantage that detailed down-core records can be constructed almost anywhere (Rutberg et al., 2000; Piotrowski et al., 2004; Horikawa et al., 2010; Böhm et al., 2015), but designing suitable leaching procedures that minimize detrital contamination remains challenging. While a few studies suggest leaching with acetic acid (AA) on carbonate rich samples is adequate (Gourlan et al., 2008, 2010), others promote acid-reductive leaching with hydroxylamine hydrochloride (HH) (Bayon et al., 2002; Gutjahr et al., 2007; Martin et al., 2010; Wilson et al., 2013). Few studies have explored systematically the effects of experimental parameters such as reagent concentration, leaching duration, solid/solution ratio on leachate ε_{Nd} and the utility of a decarbonation step (Wilson et al., 2013; Wu et al., 2015; Blaser et al., 2016).

To date, the primary concern has been designing laboratory procedures to generate authigenic ε_{Nd} records free from detrital contamination. Traditional views assume *a priori* that authigenic phases record bottom water ε_{Nd}; deviations from bottom water signatures are often inferred to reflect problems with the extraction process, particularly in bulk sediment leaching studies (Gutjahr et al., 2008; Elmore et al., 2011; Wilson et al., 2013; Huang et al., 2014). However, the recently proposed "bottom up" perspective (Abbott et al., 2015b) calls for rethinking of how authigenic ε_{Nd} is related to bottom water. Nearly all the core-top studies in the Pacific Ocean (Vance et al., 2004; Horikawa et al., 2011; Ehlert et al., 2013; Molina-Kescher et al., 2014a) and several others in the Atlantic Ocean (Elmore et al., 2011; Tachikawa et al., 2014) reported ε_{Nd} extracted from foraminifera and fish debris that were different from bottom water, and it seems unreasonable to attribute all these cases to extraction bias, as in some cases of Fe–Mn leachates.

Early on, Palmer (1985) and Palmer and Elderfield (1985) suggested that the diagenetic nature of Fe–Mn oxyhydroxide coatings on foraminiferal tests implied that they register pore water ε_{Nd}. Similarly, Toyoda and Tokonami (1990) concluded that the REEs in sedimentary biogenic phosphates were dominantly derived from pore water rather than bottom water. While it was well recognized earlier that authigenic phases are actively engaged in the early diagenetic cycle of Nd (Elderfield and Sholkovitz, 1987; Sholkovitz and Elderfield, 1988; German and Elderfield, 1989; Sholkovitz et al., 1989, 1992; Haley et al., 2004), the implications of these findings have rarely entered the discussions on the application of authigenic ε_{Nd} in paleoceanography (Kraft et al., 2013; Tachikawa et al., 2014).

Abbott et al. (2015b) advanced understanding beyond the earlier inferences by showing that dissolved Nd in pore waters had ε_{Nd} that differed from bottom water in the Northeast Pacific. The pore water data on Nd concentrations require a net flux from the sea floor into bottom waters at these sites. Abbott et al. (2016) further found that at their sites bottom water is the least important reservoir in terms of concentration in the early diagenesis of Nd and

suggested that trace detrital minerals can significantly influence the authigenic and pore water ε_{Nd} (Abbott et al., 2016). Similarly, other pore water studies pointed out that the diagenesis of detrital sediments, including volcanic ash, can lead to enrichment of Nd in pore water, which in turn exchanges Nd with authigenic Fe–Mn and phosphate phases (Caetano et al., 2009; Schacht et al., 2010). These findings cast doubt on the traditional interpretation of authigenic ε_{Nd} as a quasi-conservative bottom water tracer and suggest that pore water and detrital sediment are involved in the formation of authigenic ε_{Nd}.

Here we examine the relationships of ε_{Nd} among authigenic phases, bottom waters, and detrital sediments in the Gulf of Alaska (GOA) from the Northeast Pacific (Fig. 1a). This is a particularly useful area to test hypotheses about bottom-up control of Nd in the ocean, because it spans the region of the oldest water masses in the global ocean, for example as reflected in low oxygen content (Fig. 1b). Given this high water mass age and the size of the North Pacific, this is an important region for carbon budgets of the global ocean and changes in water masses here may have global biogeochemical consequences. This poorly understood region also presents some challenges; bulk sediments include Nd-bearing authigenic and detrital mineral phases with a broad range of reactivities (Wilson et al., 2013; Abbott et al., 2016), and developing a leaching procedure that separates authigenic Fe–Mn oxyhydroxides from bulk sediments requires distinguishing detrital sediment components, including potentially reactive juvenile volcanic materials, from authigenic components.

We explore rigorously the methodological effects of reagent type, concentration and leaching duration on leachate ε_{Nd} and optimized a combination of experimental parameters to extract Nd from authigenic phases. We test this procedure in a set of core-top and volcanic ash samples to identify the sources of Nd in leachates. We evaluate how detrital contamination may affect leaching results, and provide methods to reliably isolate the uncontaminated ε_{Nd} signature from authigenic Fe–Mn oxyhydroxides in these complex sediments. We find systematic offsets of authigenic ε_{Nd} in GOA core-top sediments relative to the ε_{Nd} signature of regional bottom waters. We propose a conceptual model relating authigenic ε_{Nd} to that of bottom water, pore water, and detrital sediment, and show that this model can explain basin-scale distributions of deep water ε_{Nd} in the Pacific, while a model of conservative water mass mixing cannot. These findings lead to a new framework for the use of authigenic ε_{Nd} as a tracer in paleoceanography that acknowledges the importance of the diagenetic cycle of Nd in the coupled ocean-sediment system (Abbott et al., 2016).

2. MATERIALS AND METHODS

2.1. Sampling

Core-top sediments stored at the Marine Geology Repository of Oregon State University (http://osu-mgr.org/) were sampled for this study (location metadata in Electronic Annex Table EA1). Water depth of these cores ranges from 125 m to 4575 m with about half shallower than 1000 m. Most of the cores, including all but one of the shallower cores, were retrieved by the EW0408 Expedition in 2004. Samples from pristine multicores were taken as close to the sediment interface as possible and were all within the upper 7 cm. The rest of the gravity and piston cores were sampled only for the top 1 cm interval.

All the core-top sediments are described as dark sandy to silty clay. GOA sediments are predominantly lithogenic (>90%) and poor in carbonate (<5%) but may contain traces of biogenic silica and organic matter (Walinsky et al., 2009; Jaeger et al., 2014). The sediment columns may include discrete volcanic ash layers and minor dispersed volcanic glasses to various degrees; most of this ash is sourced from the volcanic centers in the Aleutian Arc and Alaska-Canada Cordillera (Scheidegger et al.,

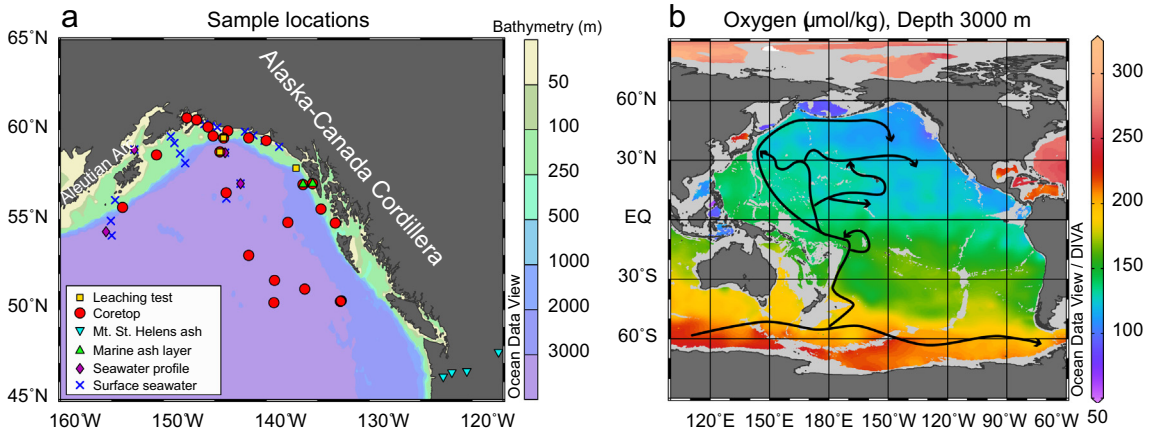

Fig. 1. Sample locations and hydrography. (a) Locations of samples, including test samples, core-top samples, marine ash layer samples and Mount St. Helens ash samples. These samples may come from the same core so there is overlap in the map. See Table EA1 for detail sampling information. Locations of the seawater profiles and surface seawater samples in the GOA (Haley et al., 2014) used in Fig. 3 are included. (b) Distribution of dissolved oxygen concentration in the Pacific from World Ocean Atlas 2013 database (Garcia et al., 2014) and major Southern Ocean deep water (Lower Circumpolar Deep Water) circulation routes entering the Pacific according to Kawabe and Fujio (2010). Fig. 1b is created using Ocean Data View (Schlitzer, 2014).

1980; Jaeger et al., 2014). Sedimentation rates are exceptionally high on the GOA margin, 5 mm/yr to 48 mm/yr (Walinsky et al., 2009), and even at ~4000 m water depth sedimentation rates are >0.1 mm/yr (Jaeger et al., 2014; Praetorius et al., 2015), suggesting that minor ash input is highly diluted by terrigenous input. No discrete ash layers were found in the upper 20 cm of the cores studied here. Rare (<1%) dispersed volcanic glasses were detected in smear slides at two sites (EW0408-25MC at 10 cm and -39MC at 20 cm); no ash was detected in other core-top sediments. All multicore tops sampled here are essentially modern, based on ^{210}Pb and ^{14}C (Walinsky et al., 2009; Davies et al., 2011; Davies-Walczak et al., 2014; Praetorius et al., 2015). Other core-top samples from archived piston and gravity cores do not have verified ages, but fill out the geographic distribution of sites. However, at each depth range there is at least one verified modern multicore top. Two down-core samples from cores EW0408-85JC and EW0408-87JC, dated using ^{14}C to late glacial time (Davies-Walczak et al., 2014; Praetorius et al., 2015) are also selected.

To further improve our understanding of the effect of volcanic ash on leachate ε_{Nd}, we sampled one ash-bearing sediment interval of core EW0408-66JC, two discrete volcanic glass layers in core EW0408-26JC and two pumice layers in core EW0408-40JC; these are all down-core samples of unknown age, and the latter four are referred to as "GOA marine ash layer" samples. Note that none of these samples are pure ash; all contain some ambient sediments. For comparison to a pure ash end member we analyzed *fresh* Mount St. Helens volcanic ash samples collected shortly after the 1980 eruption at four locations in the State of Washington, United States. Further sampling information can be found in Table EA1.

2.2. Developing leaching tests to extract authigenic ε_{Nd}

We tested various leaching methods on two modern core-top samples (EW0408-84MC and EW0408-88MC), two late-glacial samples (EW0408-85JC and EW0408-87JC, sites correspond to those of EW0408-84MC and -88MC, respectively) and one ash-bearing sample (EW0408-66JC). Collectively, these are referred as "test samples" (Fig 1a). All leach tests started with fresh bulk samples (i.e., no sequential leaching or decarbonation). This choice is made for two reasons: (1) Wilson et al. (2013) showed that it is highly likely a decarbonation step in a sequential leaching procedure could lead to considerable detrital contamination in final leachates; (2) cleaned and uncleaned planktonic foraminiferal ε_{Nd} are typically identical and therefore Nd from the carbonate lattice of fossil shells is insignificant compared to Nd in Fe–Mn coatings (Palmer, 1985; Haley et al., 2005; Roberts et al., 2012; Tachikawa et al., 2014). These published results suggest sequential leaching and a decarbonation step will not only lead to loss of authigenic Nd but also increase the risk of contamination, and is not necessary.

For extraction of authigenic components we explored differences between acidic (acetic acid; AA) leaching and acid-reductive (hydroxylamine hydrochloride acidified by acetic acid; HH) leaching. For the AA tests, we made a reagent stock of 3.33 M acetic acid buffered to pH ≈ 4 by sodium acetate. For the HH tests, we made a reagent stock of 0.053 M hydroxylamine hydrochloride, 2.62 M acetic acid and buffered to pH ≈ 4 by sodium hydroxide.

In the AA tests (AA1–AA3) we fixed the reagent concentration at 10% (v/v of the stock solutions listed above; diluted with Milli-Q® water; MQW, 18.2 Ω) while increasing the leaching duration from 3 h to 18 h. We performed two sets of HH tests. In the first experiment (HH1–HH6) we set the leaching duration to 0.5 h but increased the reagent concentration from 5% to 50%. In the second experiment (HH7–HH11), we fixed the HH reagent concentration at 50% and varied the leaching duration from 1 h to 48 h. This design illustrates how integrated leaching intensity controlled by either leaching duration or reagent concentration affects leachate ε_{Nd}. All experimental parameters are reported in Table EA2.

For each test, 1 g freeze-dried sediments were rinsed with MQW three times in centrifuge tubes. After supernatant removal, diluted reagents (7 ml in AA tests or 8 ml in HH tests, Table EA2) were added into the tubes, which were then left on a Labquake™ Tube Rotator (Thermo Scientific) for reaction. After waiting for the reaction time specified for each experiment, the samples were centrifuged (4000 rpm, 10 min), supernatant leachates were collected by pipette and filtered through 0.45 μm nuclepore syringe filters with polyethersulfone membranes, and then were evaporated to dryness. Next, concentrated nitric acid was added to the leachate samples to break down organic compounds. A small aliquot was then extracted for elemental analyses, and the remaining solution was converted to a dominantly chloride solution using 6 M HCl for ion exchange chromatography and isotopic analyses.

For reasons described in the discussion, we applied method HH4 to an array of other core-top samples from the region (Table EA1). Dry weights of some core-top samples were slightly below 1 g because of limitations of sample availability. In any case, no less than 0.8 g was used and we adjusted the volume of reagent accordingly to fix the solid/reagent ratio at 1 g/8 ml (Wilson et al., 2013). Finally, to evaluate the potential effect of dispersed trace volcanic ash on leachate ε_{Nd}, we applied method HH4 to the Mount St. Helens fresh volcanic ash and GOA marine ash layer samples, and in this case the dry weights of samples were fixed at 1 g.

For bulk sediment analyses, separate samples from the same cores and depths as the five leaching test samples were freeze dried and then digested using a mixture of HF-HNO_3-HCl in a CEM MARS-6 microwave oven, following our published procedure (Muratli et al., 2012).

2.3. Analytical methods

2.3.1. Elemental concentrations

Major elements (Al, Ca, K, Mg, Fe and Mn) and several minor elements (Ba, Co, Cu, V and Sr) were analyzed on a Teledyne Leeman Prodigy ICP-OES at the W.M. Keck Collaboratory for Plasma Spectrometry of Oregon State University. Procedural blanks for these elements were

always below method detection limits and 2σ uncertainties were <5% of measured values. Trace elements Cr, Ni, Sc, U, Y, Zn and REEs were analyzed on a Thermo VG ExCell quadrupole ICP-MS in the same laboratory. Samples, standards and blanks were all spiked and normalized with internal standards (^{209}Bi, ^{187}Re and ^{103}Rh). For REEs, procedure blanks were <0.5% and 2σ uncertainty was ~3%. Repeated measurements of digestion standards (PACS-2 and an in house standard) yielded <3% (1σ) external precision for REEs and <6% for all the other elements. All elemental concentrations are reported as total extracted elemental mass normalized to the dry weight of sediment leached (i.e., ng element/g sediment).

2.3.2. Nd and Sr isotopes

Neodymium and Strontium were isolated from other elements in leachates using ion exchange chromatography columns. Neodymium separation employed Ln-spec™, following Abbott et al. (2015b). Strontium was purified using Sr-spec™, following Abbott et al. (2016). Total procedure blanks for Nd and Sr isotope analyses were 0.13 ± 0.07 ng Nd and 6 ± 2 ng Sr, which are negligible (<0.5% for both) relative to sample yields.

Neodymium and Strontium isotopic compositions were analyzed on a *Nu Instruments* MC-ICP-MS in the Keck Collaboratory at Oregon State University. Instrumental mass fractionation was accounted for by normalizing to ^{146}Nd/^{144}Nd = 0.7219 and ^{86}Sr/^{88}Sr = 0.1194 following exponential laws (Steiger and Jäger, 1977; O'Nions et al., 1979). ^{143}Nd/^{144}Nd and ^{87}Sr/^{86}Sr ratios were then normalized to the accepted values of their respective standards, namely 0.512115 for JNdi-1 and 0.710245 for NBS 987. 2σ uncertainties of the JNdi-1 and NBS 987 standards from repeated analyses were ±0.000018 (n = 397) and ±0.000049 (n = 671) respectively. In-house standards were used to monitor external precision for ^{143}Nd/^{144}Nd and ^{87}Sr/^{86}Sr and their long-term 2σ uncertainties were ±0.000019 (n = 350) and ±0.000049 (n = 461). Neodymium isotope composition was expressed in ε-notation (normalized to the present Chondritic Uniform Reservoir value of 0.512638 (Jacobsen and Wasserburg, 1980)). The 2σ external reproducibility in this unit is ±0.37, which is used to create uncertainty bars in the plots.

3. RESULTS

3.1. Nd and Sr in leaching tests and bulk digestions

In the AA tests, the amounts of extracted Nd and leachate ε_{Nd} are similar for each individual sample (within analytical uncertainty for the latter) (Fig. 2, Table EA3). In the HH tests, Nd concentrations increase as extractions become more aggressive, particularly from HH1 to HH4 during which the concentrations more than doubled. Apart from an initial drop of ~1 ε from HH1 to HH3 in EW0408-88MC, leachate ε_{Nd} of all HH tests are essentially constant for each individual sample. Except for HH1 and HH2, AA leaches extract Nd that were 11% to 75% of the HH leaches. The similarity of ε_{Nd} between the AA and HH leachates, with the exception of core-top EW0408-88MC, suggests that a significant amount of Nd that is HH-extractable is also AA-extractable. This finding is consistent with suggestion of Wilson et al. (2013) that the decarbonation step in sequential leaching procedures is not needed.

In the AA tests, concentrations of Sr do not vary as systematically as those of Nd (Fig. 2, Table EA3). In the HH tests, the variations of Sr concentrations are within 20% of the average for all samples except core-top EW0408-88MC, which saw an overall two-fold increase from HH1 to HH6. Further, ^{87}Sr/^{86}Sr is essentially constant throughout the tests for each individual sample.

On average, leachates extract ~1% of Nd and ~10% of Sr relative to the total amounts measured from complete digestions of bulk sediments (Fig. 2, Table EA3). Bulk sediments have distinctively high ε_{Nd} and low ^{87}Sr/^{86}Sr values compared to the leachates. All bulk sediment ε_{Nd} values are similar (+3.1 to +4.9) and so are bulk ^{87}Sr/^{86}Sr (0.70661–0.70698) with the exception of a low ^{87}Sr/^{86}Sr value of the ash-bearing core EW0408-66JC (0.70571).

3.2. Nd and Sr in core-top leachates

We applied the HH4 leaching procedure (0.5 h, 30% HH, 1 g dry sample in 8 ml reagent, pH ≈ 4) on a larger array of core-top samples to assess spatial and water-depth variability of leachate ε_{Nd} values relative to measured seawater values in the GOA (locations in Fig. 1a and results in Table EA3). Overall, core-top leachate ε_{Nd} is within the range of −2.0 to +1.5 (Fig. 3a). Shallower than 500 m the average value is −0.1 (1σ = 0.7, n = 10, range from −1.5 to +0.9). At two sites near 700 m, ε_{Nd} is between −1.5 and −1.0. At about 1500 m ε_{Nd} ranges from −1 to 0. At depths greater than 3000 m most samples cluster between −1.5 and −1.0 though two leachates have values as high as +1.0. The ε_{Nd} of core-top leachates are almost always ~2 ε higher (more radiogenic) than GOA seawater at equivalent depths (Haley et al., 2014), although the spatial heterogeneity of seawater ε_{Nd} at depths <200 m makes comparison difficult at shelf depths (Fig. 3a). Below 1500 m, leachate ε_{Nd} from piston and gravity core-tops are similar (with the exception of two samples bellow 3000 m) to multicore tops from the same depth range that are verified to be modern, suggesting the vertical distribution described here is a robust feature.

Unlike ε_{Nd}, core-top leachate ^{87}Sr/^{86}Sr varies significantly with water depth (Fig. 3b). Shallower than 200 m, leachate ^{87}Sr/^{86}Sr is in the range of 0.70729–0.70905. As depth increases, leachate ^{87}Sr/^{86}Sr becomes significantly less variable and it converges to modern seawater value (0.7091792 ± 0.0000021) (Mokadem et al., 2015) at depths greater than 3000 m. Low abundance (<5%) of marine carbonate in GOA sediments makes it possible to correct leachate ^{87}Sr/^{86}Sr for contributions of Sr from carbonate dissolution during extraction. We assume that all extracted Ca is from biogenic carbonates (thus the corrections represent maximal offsets from measured leachate values) and then use a Sr concentration of 1200 ppm and modern seawater ^{87}Sr/^{86}Sr in marine carbonate to compute the carbonate-free leachate ^{87}Sr/^{86}Sr (Fig. 3b). Details are presented in the Electronic Annex Section 1. Such corrections

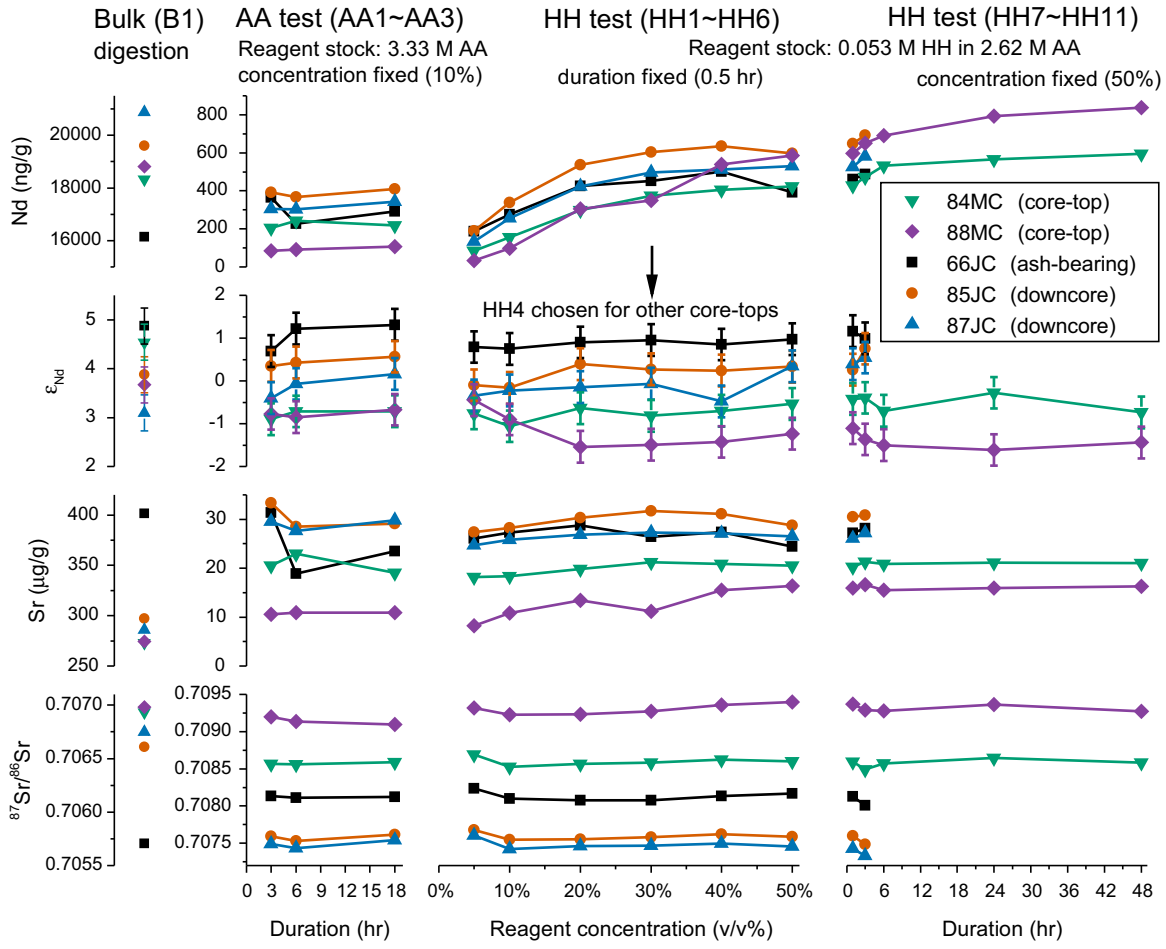

Fig. 2. Results from leaching tests. Each datum represents a distinct test, and all tests were done on fresh samples. Bulk digestion (B1) reflects the composition of the total sediment. Partial leaching tests of varying intensity are based on acetic acid (AA) or hydroxylamine hydrochloride (HH). Tests AA1–AA3 and HH7–HH11 examine the effect of increasing leach duration with constant reagent concentration. Tests HH1 to HH6 examine the effect of increasing reagent concentration over a fixed time of 30 min. Tests HH9 to HH11 were only done on the two modern core-top samples (EW0408-84MC and EW0408-88MC). Elemental concentrations are reported as total extracted elemental mass normalized to dry weight of sediments; note that plot scales for bulk digestions are different from those of leachates. Experimental parameters are reported in Table EA2 and data are reported in Table EA3.

make core-top leachate $^{87}Sr/^{86}Sr$ from shallow water sites deviate even more from the known seawater value, but have little effect at depth (particularly bellow 3000 m).

3.3. Nd and Sr in ash leachates

Leachates from the four Mount St. Helens fresh ash samples (erupted in 1980) have very similar ε_{Nd} values (+6.2 to +6.4) and the $^{87}Sr/^{86}Sr$ of ash leachates are also in a narrow range (0.70348–0.70459), except for one sample from Spokane (0.70608) (Table EA3). Whole-rock digestion of volcanic materials erupted in the same 1980 event yielded ε_{Nd} of +5.8 and $^{87}Sr/^{86}Sr$ of 0.703607 (Halliday et al., 1983).

The $^{87}Sr/^{86}Sr$ of the four GOA marine ash layer leachates are very similar to each other (0.70829 –0.70859), but their ε_{Nd} values differ (−0.6 to +3.1) (Table EA3). Compared to the Mount St. Helens ash samples, these marine ash leachates have much lower ε_{Nd} and higher $^{87}Sr/^{86}Sr$. Note, however, that the marine ash layer samples are not pure ash, but are natural mixtures of ash and ambient sediment.

3.4. REEs in leaching tests, bulk digestions, core-top and ash samples

Rare Earth Element patterns normalized to Post-Archean Australian Shale (PAAS) (McLennan, 1989) and praseodymium (Pr) are highly consistent across leaching tests and core-top extractions (Fig. 4, Table EA3). Leachates are enriched in middle REEs (MREEs) relative to both light REEs (LREEs) and heavy REEs (HREEs) and except for one core-top sample (Y70-4-56) all the other extractions have negative Ce anomalies. Fully digested GOA bulk sediments are characterized by a flatter yet relatively LREE-depleted pattern (Fig 4a). All the test and core-top leachates and digestions have positive Eu anomalies. Leachates of the dacitic Mount St. Helens ash samples

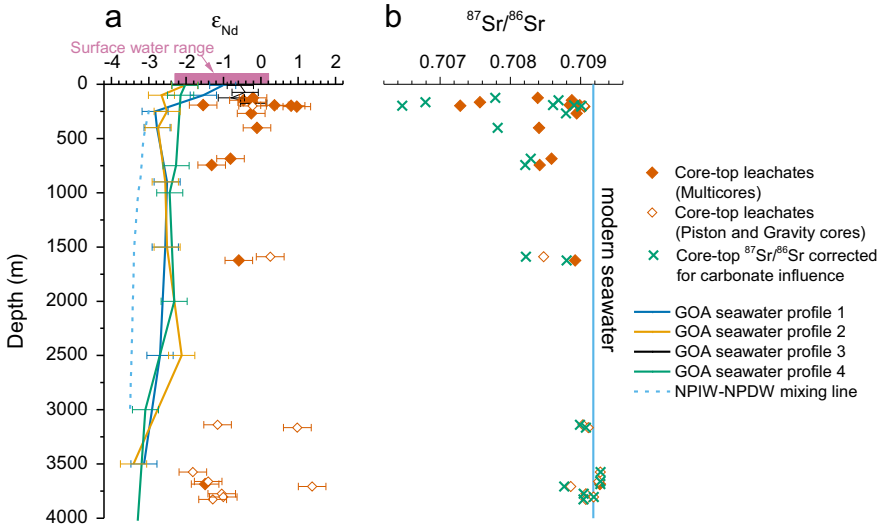

Fig. 3. (a) ε_{Nd} and (b) $^{87}Sr/^{86}Sr$ of core-top leachates (diamonds with analytical uncertainty bars), surface seawater ε_{Nd} (pink bar) and water column ε_{Nd} profiles from the GOA (solid lines with uncertainty) (Haley et al., 2014). Multicore tops that are verified to be modern are marked by solid diamonds. Piston and gravity core-tops that do not have verified ages are marked by hollow diamonds. The similarity of leachate ε_{Nd} between piston and gravity cores and multicores below 1500 m at the same depth range (with the exception of two samples) suggests the vertical distribution is a robust feature. Dashed line is a prediction based on conservative mixing between North Pacific Intermediate Water (NPIW) and North Pacific Deep Water (NPDW) (Abbott et al., 2015b). Modern seawater $^{87}Sr/^{86}Sr$ value of 0.7091792 is from Mokadem et al. (2015). The $^{87}Sr/^{86}Sr$ of core-top leachates corrected for carbonate contributions are also shown as X symbols (see the Electronic Annex Section 1). (For interpretation of the references to colour in this figure legend, the reader is referred to the web version of this article.)

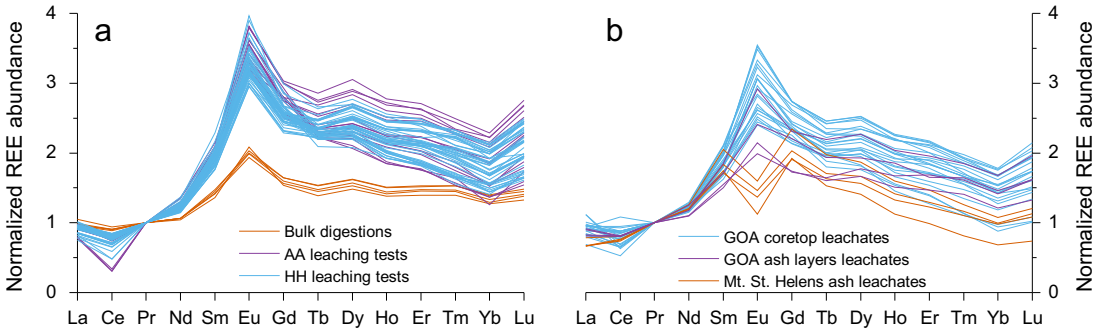

Fig. 4. PAAS- (McLennan, 1989) and Pr-normalized REE patterns of bulk sediments and leachates in this study. Panel (a) shows AA leaching tests (purple), HH leaching tests (blue) and bulk digestions (vermillion). Panel (b) shows HH4 leaches of GOA core-tops (blue), Mount St. Helens ash leachates (vermillion) and GOA marine ash layer leachates (purple). (For interpretation of the references to colour in this figure legend, the reader is referred to the web version of this article.)

have strong PAAS normalized negative Eu anomalies (Fig 4b). Leachates of GOA marine ash samples (which are mixtures of ash and ambient sediment), however, show positive Eu anomalies and MREE enrichment similar in shape to the GOA core-top leachates (Fig 4b).

4. DISCUSSION

4.1. Insensitivity of leachate ε_{Nd} to experimental parameters and its implication for extracted phases

Within the ranges of tested leaching parameters, ε_{Nd} is insensitive to reagent type, concentration and leaching duration (Fig. 2). This consistent behavior of ε_{Nd} contrasts sharply to Nd concentrations, which increase continuously with greater leaching intensity in the HH tests (Fig. 2). These data suggest that increasing leaching intensity extracts more Nd of relatively fixed ε_{Nd} from a dominant (plausibly authigenic) phase. The observed decoupling between ε_{Nd} and Nd concentration precludes the possibility that leachate ε_{Nd} represents mixing of two or more phases with distinct ε_{Nd} (for example, authigenic and detrital phases), unless these phases release Nd proportionally during extraction. This proportional release hypothesis would require that the contributing phases have essentially identical reaction kinetics, which is implausible (Wilson et al., 2013).

The consistency of REE patterns (Fig. 4) in leaching tests and additional core-top leaches, and their distinct difference from bulk sediment digestions, further support the

hypothesis that only one dominant phase was extracted that has a distinct MREE bulge pattern. The relative stability of $^{87}Sr/^{86}Sr$ in leaching tests (Fig. 2) also agrees with this hypothesis, although dissolution of carbonates may influence the Sr signals, unlike the Nd (and ε_{Nd}) signals.

We choose the HH4 procedure as our standard method for core-top samples because our test results show this extraction method reflects the least intensive leaching beyond which no change of ε_{Nd} was observed (Fig. 2). This choice is arguably arbitrary, but HH4 procedure consistently yields enough Nd for isotopic analysis from ~1 g samples. Further increasing leaching intensity increases the potential risk of contaminating the leachate with other phases (e.g., detrital sediment), although we did not observe any significant changes in leachate ε_{Nd} even with the two stronger leach recipes of HH5 and HH6.

4.2. Nd bearing phases in sediment

The dominant phase extracted in test and core-top leachates yields ε_{Nd} clearly offset from measured bottom water ε_{Nd} (Fig. 3a). To consider whether this offset indicates widespread detrital contamination of leachate Nd, we examine the possible sources of Nd to leachates in sediment. Potential candidates for Nd in the leaches are authigenic Fe–Mn coatings, biogenic materials and detrital sediments. In this study we define detrital sediment as the non-authigenic and non-biogenic fraction of the sediment and in particular refer to the aluminosilicate fraction of the sediment, including both eroded terrestrial materials and volcanic ash.

All the test and core-top leachates have MREE enriched patterns typical of Fe–Mn oxyhydroxide (Gutjahr et al., 2007), suggesting this phase was principally extracted (Fig. 4). Biogenic carbonate may harbor REEs but Nd in carbonate lattice is negligible compared with Nd in Fe–Mn coatings (Shaw and Wasserburg, 1985; Palmer, 1985; Haley et al., 2005; Roberts et al., 2012; Tachikawa et al., 2013, 2014). Given that GOA sediments are poor in carbonates (<5%) (Walinsky et al., 2009; Jaeger et al., 2014), it is unlikely that carbonate contributes significantly to leachate Nd, a suggestion supported by the fact that REE pattern extracted from planktonic carbonate is typically more enriched in HREEs (Palmer, 1985; Haley et al., 2005; Freslon et al., 2014; Molina-Kescher et al., 2014a). Biogenic apatite, such as fish debris, also accumulates REEs postmortem in sediment and is also considered an authigenic archive (Martin and Haley, 2000), but there is no visual evidence of its significant presence in our samples and it is unlikely our weak leaching method can significantly attack apatite (Martin et al., 2010; Horikawa et al., 2011). There are very few studies on REEs and ε_{Nd} associated with other biogenic phases such as opal, organic matter and barite, and they are relatively rare in sediments outside of the highly productive fjords in the GOA (Walinsky et al., 2009). Since we do not use the specific reagents that target these biogenic phases (Jones et al., 1994; Martin et al., 1995; Freslon et al., 2014), we do not consider their contribution to leachate Nd to be important. Moreover, organic matter typically has more LREE-enriched (Freslon et al., 2014) and opal more HREE-enriched patterns (Akagi et al., 2011; Xiong et al., 2012) than do our test and core-top leachates, suggesting that these biogenic materials are not significant sources of leached Nd in our samples.

Because the detrital sediment includes Nd-bearing components of different reactivities and distinct isotopic compositions (McLennan et al., 1993; Wilson et al., 2013; Abbott et al., 2016), comparing leachates to bulk sediment digestions gives limited insight into detrital contamination. The same can be said for comparison of leachate to operationally defined "detrital residue" after sequential extractions (Bayon et al., 2002). Separate analysis of the various detrital components may be more insightful, but in practice these detrital components cannot be physically or chemically isolated easily. Instead, we employ geochemical provenance tracers (McLennan et al., 1993) to constrain possible inputs from various detrital end members. This approach assumes that in the leaches, Nd is proportional to its relative concentrations and reactivities in the individual detrital components.

The GOA collects mainly terrestrial sediments from the Alaska-Canada Cordillera with a minor volcanic ash component mostly from the Aleutian arc (Fig. 1) (Plank and Langmuir, 1998; Nokleberg et al., 2000; Jaeger et al., 2014). The isotopic characteristics of the terranes from Alaska-Canada Cordillera are diverse: the ε_{Nd} and $^{87}Sr/^{86}Sr$ range at least from −25 to +10 and 0.702 to 0.709 respectively (Samson et al., 1989, 1990, 1991a,b; Farmer et al., 1993). Aleutian arc volcanic rock and ash have much narrower distributions of ε_{Nd} and $^{87}Sr/^{86}Sr$, typically within +7 to +9 and 0.702 to 0.704 respectively (Turner et al., 2010; Hildreth and Fierstein, 2012; Kelemen et al., 2014). Although the Aleutian arc lavas are mainly basaltic and andesitic (Kelemen et al., 2004, 2014), volcanic ash depositions in the GOA are more evolved and predominantly rhyolitic (Pratt et al., 1973; Scheidegger et al., 1980; Cao and Arculus, 1995). Rhyolitic ash is the least reactive of these potential ash sources because of its high acidity (Wolff-Boenisch et al., 2004). Based on ε_{Nd} alone the argument in Section 4.1 precludes volcanic material as the dominant phase directly extracted in our test and core-top leachates.

Finally, it is worth considering the potential effect of "preformed" authigenic Fe–Mn oxyhydroxides that may have been delivered to marine sediments by aeolian particles and river/glacial meltwater sediments (Bayon et al., 2004; Poulton and Raiswell, 2005; Kraft et al., 2013). The extremely high sedimentation rate (5 –48 mm/yr) in the GOA (Walinsky et al., 2009) implies exceptionally high erosion and transport rates (Gulick et al., 2015). GOA sediments are mostly glaciogenic (Jaeger et al., 2014), which typically carry much less preformed phases than river borne sediments (Poulton and Raiswell, 2002). The short residence time in very small floodplains, cold temperature and large grain size (Jaeger et al., 2014) are all unfavorable for significant Fe–Mn oxyhydroxide formation during transport (Poulton and Raiswell, 2005). Indeed, Mn, Nd (and to some extent Fe) extracted from deeper core-top sediments (>3000 m) are four to ten-fold higher than Mn and Nd extracted from shallower sediments (Table EA3). These data suggest the extracted Fe–Mn phases are formed *in situ* in the marine realm rather than being transported from

elsewhere. Moreover, it seems unlikely that preformed Fe–Mn oxyhydroxides could survive the redox cycling during early diagenesis without being converted to marine authigenic phases (Kraft et al., 2013). And if such preformed oxides are resistant to diagenesis, it is then doubtful that they would be mobilized in our mild leaches of 0.5 h. For these reasons, we assume that we do not need to consider preformed oxides as a distinct reactive phase.

4.3. The major and trace element geochemistry of leachates

Elemental distributions in leachates can be used to fingerprint the phases extracted (Gutjahr et al., 2007; Gourlan et al., 2010). Here we compare the major and trace element geochemistry of HH4 leachates, including the five test samples and all the core-top leachates, to that of selected authigenic and detrital end members (Fig. 5, GOA geochemical data are reported in Table EA3). Such comparisons are necessarily complicated by possible re-adsorption and non-uniform reaction kinetics during lab extractions (Wilson et al., 2013), so our strategy is to use a multi-faceted approach (leaching tests, major and trace element geochemistry, kinetic mineral dissolution rates, isotope systematics) to derive a conclusion consistent with all observations.

The range of elemental concentrations in potential authigenic end members is constrained by published data from Fe–Mn crusts and nodules, planktonic foraminiferal extractions and published Fe–Mn leachates that are considered to be free from detrital contamination. The implicit assumption, which is borne out by our data compilation, is that the authigenic Fe–Mn phase has a characteristic geochemistry that can be compared with known values elsewhere. We consider not only detrital sediment in the averaged sense (i.e. bulk sediment or operationally defined detrital residue), but also various detrital components of distinct geochemistry and reactivity. Aleutian volcanic products (basaltic and andesitic lavas and rhyolitic and dacitic ashes) will serve as the volcanic detrital end members and the Upper Continental Crust (UCC) will represent the continental sourced detrital materials. The bulk sediments of the GOA, the Aleutian and Alaska subducting sediment composites, the Mid-Ocean Ridge Basalt (MORB) and other sources will be used as detrital end members when necessary. References to these end members are listed in the caption of Fig. 5.

Fe–Mn crusts and nodules, uncleaned planktonic foraminifera and published Fe–Mn leachates have similar Al/Nd ratios, on the order of 10^1 to 10^2. Our HH4 leachates are within the range of these values (Fig. 5a). The Al/Nd of detrital end members are one to two orders of magnitude higher than all the authigenic phases.

The detrital end members also have low Mn/Fe (<0.1) and Nd/Fe (<0.001). Our HH4 leachates have much higher Mn/Fe and Nd/Fe (Fig. 5b), which are unlike detrital components but similar to known authigenic end members. Decarbonated leachates are separated from other authigenic extractions by having Mn/Fe <0.1, suggesting preferential loss of Mn-phases, perhaps Mn-oxides and Mn-carbonates during decarbonation (Roberts et al., 2012; Wilson et al., 2013).

For most elements, ratios to Nd in HH4 leachates are proportional (approximately 1:1) to ratios in authigenic Fe–Mn crusts and nodules (Fig. 5c). An exception to this rule is the apparent enrichment of alkali-alkaline earths (Ca, Mg, Sr, and perhaps Ba), K, and U in HH4 leachates. These anomalies reflect additional sources such as carbonate (Ca and Sr), biogenic barite (Ba), sea salts (K and Mg) and authigenic U phases, which have little or no effect on leachate ε_{Nd}.

Enrichment factors, i.e., $\left(\frac{(\text{element}/\text{Nd})_{\text{sample}}}{(\text{element}/\text{Nd})_{\text{detrital endmember}}}\right)$, of the first series transitional metals in HH4 leachates (normalized to Katmai rhyolitic ash from the Aleutian Arc in Fig. 5d and other detrital end members in Fig. EA1 of the Electronic Annex Section 2) show close similarity of leachates to Fe–Mn crusts and nodules (for example, relative enrichment of Mn, Co, Ni, Cu, Zn).

Finally, REE patterns can help to diagnose the underlying geochemical processes, and we examine the indices HREE/LREE ([Yb + Lu]/[Pr + Nd]; PAAS normalized concentrations) and MREE* (2[Tb + Dy]/[Pr + Nd + Yb + Lu]) (Martin et al., 2010; Molina-Kescher et al., 2014a) (Fig. 6). Seawater, pore water, Fe–Mn crusts and nodules, planktonic foraminifera, fish debris, published Fe–Mn leachates from wide spatial and temporal ranges, all fall on the same broad trend (dash line). We call this the "authigenic-pore water array." The existence of this array suggests that the processes fractionating REEs in seawater, pore water and authigenic phases are mechanistically related, possibly reflecting the surface chemistry of authigenic phases and mineral-organic matter-water interactions (Byrne and Kim, 1990; Sholkovitz et al., 1994; Bau et al., 2013; Schijf et al., 2015).

In contrast, REE data from detrital sediments and their plausible end member components all fall on a roughly orthogonal trend that we call the "detrital array" (solid lines). This array results from mixing of continental crust and mantle derived materials. Here mantle materials are represented by MORB and continental crustal materials UCC and PAAS (McLennan, 2001) (Fig. 6). The trend in the detrital array reflects the differential partitioning of the REEs during partial melting (McLennan, 1989; White, 2013): LREEs are less compatible than MREEs and HREEs because of greater ionic radii (with the exceptions of Ce and Eu but they are not included in the MREE* and HREE/LREE indices). As a result, continental crust is more enriched in LREEs relative to the mantle and consequently has lower values of both the MREE* and HREE/LREE indices.

The identification of these two nearly orthogonal trends helps to differentiate the processes responsible for the formation of the phases of interest, i.e., low-temperature aqueous processes for authigenic phases and high-temperature igneous processes for detrital phases. Our HH4 leachates fall within the range of Fe–Mn crusts and nodules and generally follow the trend of the authigenic-pore water array. They certainly do not follow the detrital array trend, and do not form mixing lines toward either the MORB or the UCC/PAAS end members (Fig. 6).

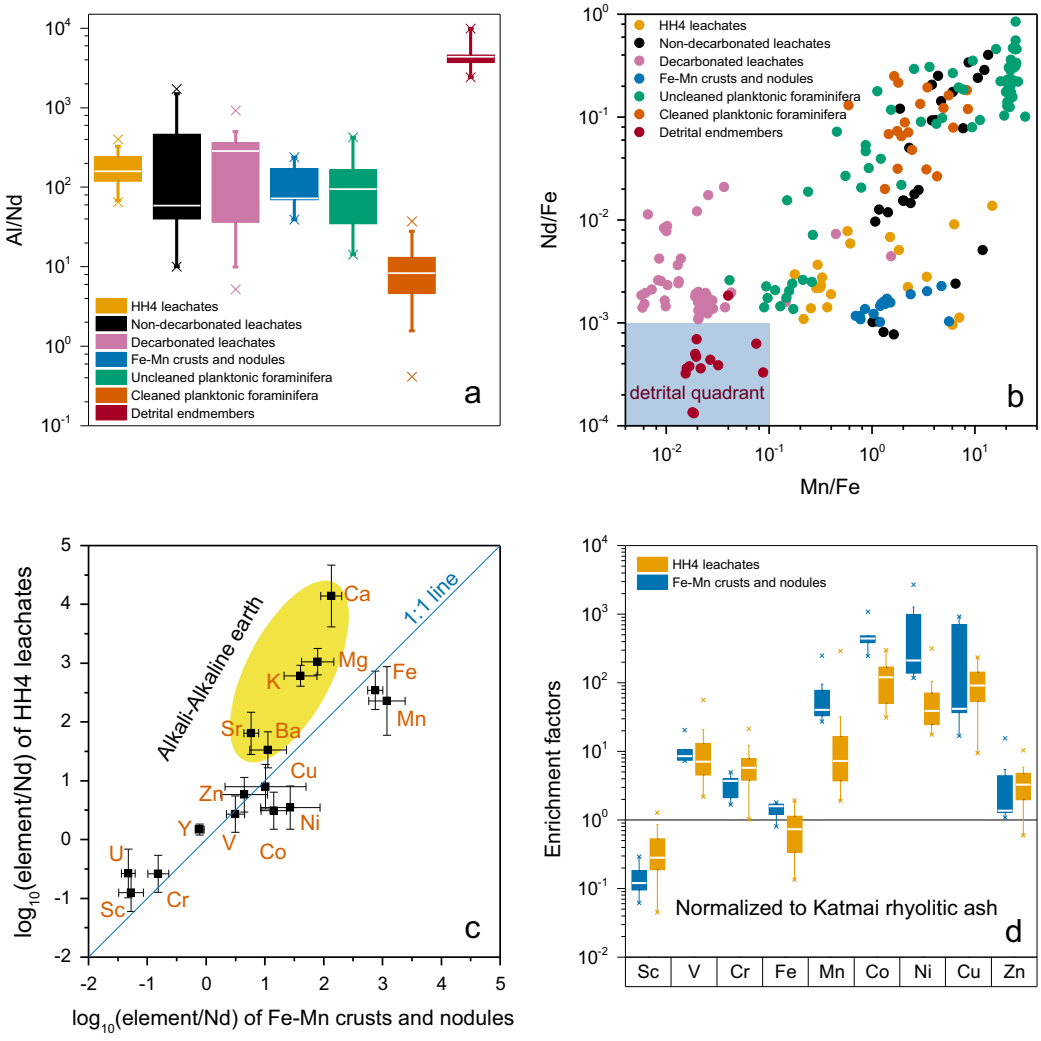

Fig. 5. Major and trace element geochemistry of HH4 leachates compared to authigenic and detrital end members (all elemental concentrations are in mass unit): (a) Al/Nd ratio (boxes span 25%-75% of the data, whiskers note the entire range of values); (b) Mn/Fe ratio versus Nd/Fe ratio; (c) $\log_{10}$(element/Nd) comparison between HH4 leachates and Fe–Mn crusts and nodules and (d) enrichment factor plot normalized to Katmai rhyolitic volcanic ash from the Aleutian Arc (boxplot setting same as in (a)). Authigenic data represent Fe–Mn crusts and nodules (van de Flierdt, 2003; Hein and Koschinsky, 2014), planktonic foraminifera (Palmer, 1985; Palmer and Elderfield, 1985; Roberts et al., 2012; Roberts and Piotrowski, 2015) and Fe–Mn leachates (Bayon et al., 2002; Gutjahr et al., 2007, 2010; Martin et al., 2010; Gourlan et al., 2010; Wilson et al., 2013). Detrital data include GOA bulk sediment, UCC (Rudnick and Gao, 2014), Aleutian basalt and andesite lavas (Kelemen et al., 2014), Katmai rhyolitic and dacitic volcanic ashes from the Southern Alaska Peninsular (Turner et al., 2010; Hildreth and Fierstein, 2012), MORB (Kelemen et al., 2014), Aleutian and Alaska subducting sediment composites as well as the global composite (Plank, 2014). The detrital quadrant in (b) contains most of the detrital end members and is defined as Mn/Fe < 0.1 and Nd/Fe < 0.001. The uncertainty bars in (c) are created using 1σ standard deviations of the HH4 leachate data and the compiled regional Fe–Mn crust and nodule data from Hein and Koschinsky (2014) respectively. Note that the variability of Fe–Mn crust and nodule data represents regional differences, and the variability on the level of individual samples may be larger.

From these elemental analyses, we conclude the phase extracted dominantly in HH4 leachates is authigenic Fe–Mn oxyhydroxide, and detrital contamination to leachate Nd is insignificant.

4.4. Kinetic mineral dissolution rates

Detrital and authigenic contributions during leaching can be further quantified by considering relative mineral dissolution rates (Table EA4, see the Electronic Annex). Mineral dissolution mechanisms can be classified as proton-promoted versus ligand-promoted, and for oxyhydroxide reductive versus non-reductive (Zinder et al., 1986; Stone and Morgan, 1987; Brantley, 2008). Chemical extractions using an acidified reducing reagent applied over a short time interval, such as our HH4 method, should represent far-from-equilibrium proton-promoted dissolution of silicate minerals and reductive dissolution of Fe–Mn oxyhydroxide (Fig. 2), and therefore short-term leaching procedures should be governed by kinetics. Indeed, we

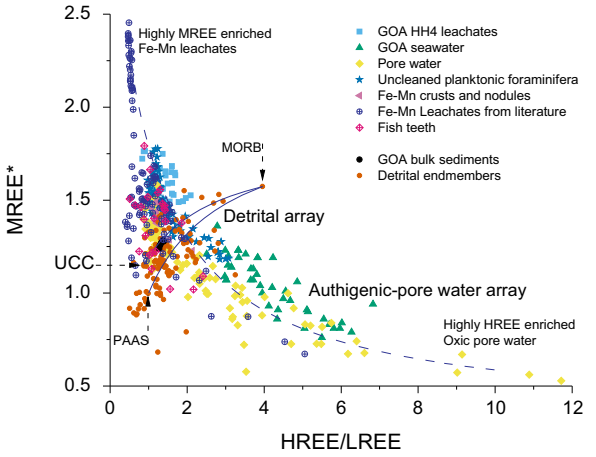

Fig. 6. HREE/LREE vs. MREE*. A mixing line between the most MREE enriched leachates (Gutjahr et al., 2010) and the most HREE enriched oxic pore water (Haley et al., 2004) reflects the "authigenic-pore water array" (dashed line). Mixing lines between MORB (Kelemen et al., 2014) and UCC (solid line) (Rudnick and Gao, 2014) or PAAS (solid line) reflect the "detrital arrays". Data include those cited in Fig.5 as well as other published values (Bayon et al., 2002, 2004; Haley et al., 2004, 2014; Martin et al., 2010; Kelemen et al., 2014; Plank, 2014; Molina-Kescher et al., 2014a; Abbott et al., 2015a; Wilson et al., 2013; Cao and Arculus, 1995).

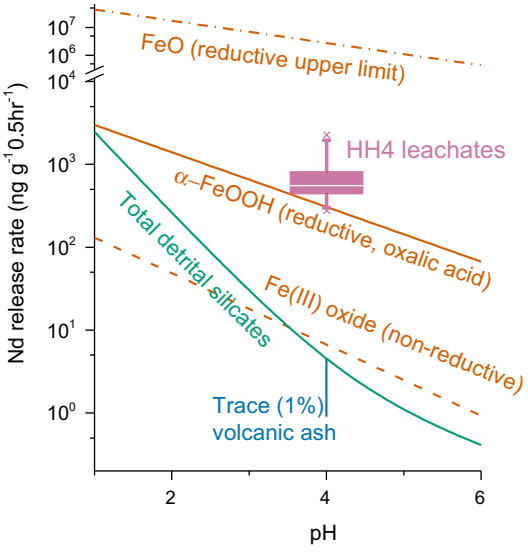

Fig. 7. Nd release rate measured in GOA HH4 leachates (pH ≈ 4, pink box; box spans 25–75% of the data, whisker notes the entire range of values) compared with Fe oxyhydroxide and detrital silicate minerals modeled using published kinetic mineral dissolution rates (lines), and pure volcanic ash based on our experiments of leaching fresh Mount St. Helens ash samples. Reductive dissolution of Fe oxyhydroxide is bounded by dissolution of FeO to the top and proton promoted non-reductive dissolution of Fe (III) oxide to the bottom (Brantley, 2008). Reductive dissolution rate of goethite (α-FeOOH) measured in 10^{-3} M oxalic acid is also shown (Zinder et al., 1986). In estimating the amount of Nd released from detrital silicates we consider the bulk mineral composition of GOA sediments and the reactivity of these minerals. Volcanic ash is present at trace level (<1%) in GOA bulk sediments. For Fe oxyhydroxide the results are reported as ng Nd released from 1 g pure minerals in 0.5 h, while for HH4 leachates, detrital silicates and volcanic ash the units are in ng Nd released from 1 g dry sediment in 0.5 h. In comparing Nd release rate from HH4 leachates to pure Fe oxyhydroxide minerals we assume the amount of authigenic phases present does not limit the reaction rate, which is supported by the observation that the release of Nd in our HH experiments seems to follow zero-order kinetics (HH6–HH11, Fig. 2). Mn oxyhydroxides are not presented here because relevant inorganic rate measurements are unknown. Details of the calculations are in the Electronic Annex Section 3. (For interpretation of the references to colour in this figure legend, the reader is referred to the web version of this article.)

found Nd concentrations from HH6 to HH9 tests increase linearly with time (0.5–6 h), suggesting zero-order kinetics. To estimate Nd extraction rates from authigenic and silicate minerals we need to know (i) the mineralogy of sediment, (ii) the relative kinetic dissolution rates of these phases under an environmental condition that is similar to our laboratory extractions (pH ≈ 4 and room temperature), (iii) the specific surface area of these minerals and (iv) the relative concentration of Nd in the source minerals.

We report pH-dependent Nd release rate calculations in Fig. 7 (details are presented in the Electronic Annex Section 3). Volcanic ash is not included in this calculation because of its rare presence; we discount the potential for ash contamination in Section 4.5. All rates are reported as ng of Nd released from 1 g of mineral/sediment in 0.5 h to facilitate comparison with our leachate data (Table EA3). We note that interpretation of these estimates is limited to an order-of-magnitude scale, as comparing kinetic mineral dissolution rate measurements with higher precision would requires more data, for example precise measurements on mineral grain sizes and surface areas, that are beyond the scope of our study (Bandstra and Brantley, 2008).

Observed Nd release rates in our HH4 leachates (220–2051 ng Nd g^{-1} 0.5 h^{-1}) fall within the theoretical bounds of reductive dissolution of Fe oxyhydroxide and are very close to the rates previously measured using oxalic acid as the reducing agent (Zinder et al., 1986). This finding is consistent with authigenic Fe–Mn oxyhydroxide being the phase extracted dominantly in HH4 leachates. Total Nd release rates from silicate minerals depend on the choice of representative mineral and specific surface area in calculation. Nevertheless, even when choosing silicate minerals of higher reactivity and with generous estimates of specific surface area, detrital Nd release rates (<10 ng Nd g^{-1} 0.5 h^{-1} in the pH range of 3.5–4.5) from these silicate minerals are two to three orders of magnitude lower than those of authigenic oxyhydroxides or our observed leach values, suggesting they can account for <1% of total Nd observed in our leachates. Given the ε_{Nd} of GOA bulk sediment is ~+5, these low levels of detrital contamination should therefore not bias leachate ε_{Nd} by more than +0.05 ε, which is within external analytical precision and thus negligible.

4.5. Estimating volcanic ash contamination

Results from leaching volcanic ash samples may provide a more accurate empirical measure of the potential effect of

ash contamination on leachate ε_{Nd} than calculations using kinetic dissolution rate can afford. The ε_{Nd} (+6.2 to +6.4) and $^{87}Sr/^{86}Sr$ (0.70348 –0.70608) of the four Mount St. Helens ash leachates (HH4 method) are very close to bulk digestion/whole rock analyses of materials erupted in the same event (+5.8 to +6.0 for ε_{Nd} and 0.703607 for $^{87}Sr/^{86}Sr$) (Halliday et al., 1983; Goldstein et al., 1984). This provides a well-constrained volcanic end member. These Mount St. Helens ash samples are dacitic, which are more reactive than the rhyolitic ash in GOA sediments (SiO_2 wt % typically >70%) (Pratt et al., 1973; Scheidegger and Kulm, 1975; Cao and Arculus, 1995) because of low acidity (Wolff-Boenisch et al., 2004). These fresh ash samples are also expected to be much more reactive than the marine dispersed ash in our samples (White and Brantley, 2003). Therefore, estimates of volcanic contamination to GOA core-top leachate based on the Mount. St. Helens end member provide an upper limit.

Neodymium extracted from the four fresh Mount. St. Helens ash samples are in the range of 90–450 ng/g in 0.5 h (Table EA3). Since the observed dispersed ash is only of trace amount (<1% wt) in GOA core-top sediments, up to 4.5 ng of Nd might be derived from ash in our core-top leaches extracted from 1 g dry sediment (Fig. 7), assuming complete and kinetically unconstrained release and proportional re-adsorption. This estimated value of 4.5 ng of Nd from dispersed ash in 1 g sediment is equivalent to 1% (±0.5%, max = 2%) of the total measured Nd in HH4 leachates. If we assume ash ε_{Nd} of +6.9 (Katmai rhyolitic and dacitic ash from Alaska Peninsular; Hildreth and Fierstein, 2012), then this ash contribution would bias our core-top leachate ε_{Nd} of about +0.07 ε (±0.04 ε, max = 0.15 ε), which is much smaller than our 2σ analytical uncertainty (0.37 ε) and negligible.

Results of leaching the four GOA down-core marine ash layer samples (two volcanic glass layers from EW0408-26JC and two pumice layers from EW0408-40JC, both containing some ambient sediment) further support the robustness of our HH4 method. Though a similar amount of Nd was extracted from these marine ash samples (276 ng/g, $1\sigma = 180$; Table EA3), the extracted ε_{Nd} (−0.6 to +3.1) and $^{87}Sr/^{86}Sr$ (0.70829–0.70859) are far different from pure volcanic signals, suggesting that ash is not the dominant source of Nd and Sr, even in ash-layer sediments. We infer that authigenic Fe–Mn oxyhydroxide coatings dominate the Nd signal leached, as in our other non-ash layer sediments. Indeed, the REE patterns of these marine ash leachates are very similar to all the other core-top leachates with distinct MREE enrichment pattern (Fig. 4b), suggesting the dominance of low-temperature aqueous geochemical processes (Fig. 6).

We can also use $^{87}Sr/^{86}Sr$ of these marine ash layer leachates to estimate ash contamination. Though these samples contain little calcium carbonate (total extracted Ca in these leachates are only ~10% of the core-top samples, Table EA3), we still correct their leachate $^{87}Sr/^{86}Sr$ for influence of carbonate dissolution. Such a correction, however, does not decrease leachate $^{87}Sr/^{86}Sr$ more than 0.0005. Using these corrected values, mixing calculations between volcanic ash (0.70371 for Katmai rhyolitic ash) and seawater (0.7091792) show no more than 25% of the non-carbonate Sr measured in these marine ash leachates can be derived from volcanic sources. The relative contribution of volcanic sources to leachate Nd must be even lower, as Fe–Mn coatings are more enriched in Nd than Sr (Gutjahr et al., 2007). We suggest these radiogenic down-core ash layer leachates may represent genuine radiogenic authigenic ε_{Nd} that results from ash diagenesis *in situ*, rather than ash contamination during our lab extractions. This is supported by previous observations that ash dissolution can lead to extreme enrichment of pore water REEs during early digenesis (Schacht et al., 2010).

Similar to the leachates from pure Mount St. Helens ash, the leachates from marine ash layers offer some constraint on volcanic contamination in our GOA core-top leachates. Even if we make a worst-case assumption the GOA core-top samples contain as much volcanic ash as the four marine ash layer samples, and the contaminating effect to leachate Nd is as high as to leachate Sr, then ash contamination still cannot account for core-top leachate ε_{Nd} that are more radiogenic than −0.5 when the 25% upper limit is used (Fig. 3a). Together, we conclude that GOA core-top leachate-bottom water ε_{Nd} differences are not the result of ash contamination.

Thus, our geochemical arguments lead to the conclusion that the dominant Nd bearing phase extracted is authigenic Fe–Mn oxyhydroxide. Detrital contamination, from all the phases considered including ash, is an insignificant source of Nd in GOA HH4 leachates. This implies that the authigenic phases have ε_{Nd} signatures distinct from bottom water (Fig. 3a). We conclude that authigenic phases register pore water ε_{Nd}. The following sections explore the consequences of this finding.

4.6. Pore water process to explain the decoupling between ε_{Nd} and $^{87}Sr/^{86}Sr$ in core-top leachates

The conclusion above implies that the deviation of core-top authigenic ε_{Nd} from bottom water ε_{Nd} (Fig. 3a) must be the results of processes happening *in situ*. We show here that this deviation can be explained by the contribution of the long-term diagenesis of detrital sediment to the *formation* of pore water and authigenic ε_{Nd}. This explanation is consistent with our observation that leachate $^{87}Sr/^{86}Sr$ (corrected for Sr release from carbonate during extraction; Figs. 3b and 8) have seawater-like $^{87}Sr/^{86}Sr$ (core-top samples >3000 m) at the same time leachate ε_{Nd} diverges systematically from bottom water values. We refer to this phenomenon as "decoupling".

Because bottom water is far more enriched in Sr over Nd relative to detrital sediments by five orders of magnitude – for example, 7 ppm Sr (Sarmiento and Gruber, 2013) and 4×10^{-6} ppm Nd (Haley et al., 2014) in seawater, compared to 306 ppm Sr and 19 ppm Nd in GOA bulk sediment – the $^{87}Sr/^{86}Sr$ signal of pore water is inherited from bottom water and is relatively insensitive to detrital inputs. In contrast to $^{87}Sr/^{86}Sr$, the ε_{Nd} of pore water is highly sensitive to sediment diagenesis. For example, a binary mixing model for pore water $^{87}Sr/^{86}Sr$ and ε_{Nd} between bottom water and detrital sediment, weighted by the composition and

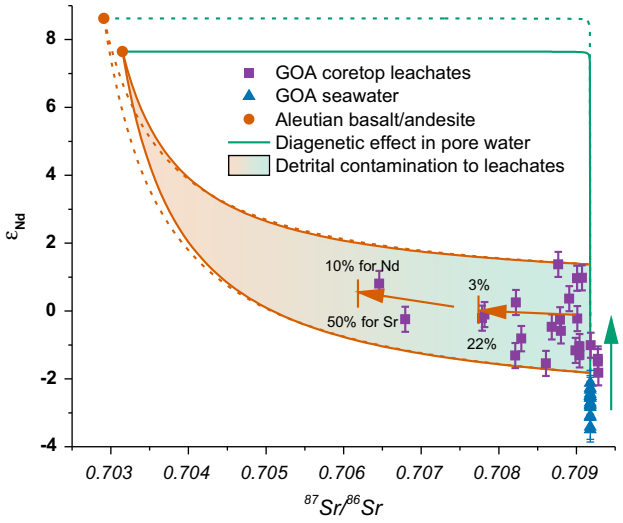

Fig. 8. The ε_{Nd} -$^{87}Sr/^{86}Sr$ isotopic systems in GOA core-top leachates. Leachate $^{87}Sr/^{86}Sr$ are corrected for the effect of carbonate dissolution (Fig. 3, also see the Electronic Annex Section 1). Green solid and dashed lines are the *in situ* mixing lines between GOA seawater and Aleutian volcanic products, representing the influence of volcanically derived components on pore water and authigenic isotopic compositions happening during sediment diagenesis. The vermilion lines and shaded region indicate the potential effects of mixing between Aleutian volcanic products and authigenic phases in the laboratory during leaching, i.e., this quantifies the effects of contamination on leachate isotopic signatures. The arrows demonstrate the directions of such processes and on the arrow heads we show the percentage volcanic contaminations to leachate Nd and Sr (non-carbonate fraction). For <3 % contamination of the Nd component during leaching, the effect on ε_{Nd} is negligible compared to analytical uncertainties. The geochemistries of the end members are: Sr = 445 ppm, Nd = 9 ppm, $^{87}Sr/^{86}Sr = 0.70315$ and $\varepsilon_{Nd} = +7.65$ for Aleutian basalt; 1035.88 ppm, 20.2 ppm, 0.70291 and +8.62 for Aleutian andesite (Kelemen et al., 2014); and 7 ppm, 4.26 ppb, 0.70918 and −2.7 for GOA seawater (Haley et al., 2014). In creating the vermillion mixing lines, authigenic $^{87}Sr/^{86}Sr$ is taken to be the same as seawater, and two authigenic ε_{Nd} end members (−1.38 and +1.83) are chosen to bracket the core-top leachate data. We use a Sr/Nd ratio of 5.7 for authigenic phases, same as in Fe–Mn crusts and nodules (Hein and Koschinsky, 2014). (For interpretation of the references to colour in this figure legend, the reader is referred to the web version of this article.)

reactivity of the sedimentary components (see the Electronic Annex Section 4), shows that the deviation of pore water $^{87}Sr/^{86}Sr$ from the seawater value (0.7091792) would not exceed our 2σ analytical uncertainty (0.000049) until >99.5% of pore water Nd is derived from sediment (Fig. 8, green lines). Volcanic materials are typically more reactive than crustal sourced materials (Elderfield and Gieskes, 1982; Jones et al., 2012; Wilson et al., 2013; Jeandel and Oelkers, 2015; Bayon et al., 2015), but are rare relative to eroded terrigenous material in the GOA. Nevertheless, the reactivity-weighted detrital ε_{Nd} is expected to bias toward volcanic values, so we choose Aleutian basalt and andesite as the reactive end members of detrital sediment to create mixing lines with seawater. Mixing lines between bulk sediment and seawater would lead to virtually the same result. Although this mixing model is quite simple, the GOA deep (>3000 m) core-top leachates fall close to this mixing trend (Figs. 3 and 8), supporting the conclusion that the deviation of authigenic ε_{Nd} from bottom water toward more radiogenic values and the observed ε_{Nd} -$^{87}Sr/^{86}Sr$ decoupling are the results of long-term sediment diagenesis within pore water, at least for this region.

The mixing model can also be used to assess the effects of contamination of ε_{Nd} and $^{87}Sr/^{86}Sr$ during the leaching process. In this case, $^{87}Sr/^{86}Sr$ is most sensitive to contamination effects (Fig. 8; vermilion lines and shaded region; two scenarios are chosen to bracket the range of core-top data), because authigenic Fe–Mn oxyhydroxide is more enriched in Nd than Sr relative to ambient detrital sediments (Gutjahr et al., 2007). This trend is orthogonal to the mixing trend that occurs naturally within pore water. Binary mixing between the authigenic phase and Aleutian volcanic products explains the observed range of isotopic values in core-top leachates (Fig. 8). Although some contamination from reactive volcanic components may explain the relative low $^{87}Sr/^{86}Sr$ in the core-top leachates, the possible contamination effect on ε_{Nd} is less than analytical precision in all cases except two shallow samples, showing that our HH4 method generally provides robust values of authigenic ε_{Nd}. We note that although some of these data could also fall in the mixing regions between bulk sediment and authigenic phases, others require the mixing of authigenic phases with volcanic components. Whichever end member is chosen as the source of contamination, the effect on leachate ε_{Nd} is insignificant for most of the samples (in particular the samples >3000 m that have seawater-like $^{87}Sr/^{86}Sr$). We favor the parsimonious argument that laboratory contamination comes primarily from the volcanic components of relatively high reactivity (Wilson et al., 2013), instead from the bulk sediment in the generic sense (which is made of components of distinct reactivity and geochemistry) (Abbott et al., 2016), but emphasize that the effects of this contamination, regardless of the end member chosen, are within analytical precision and thus

negligible in our experiments except the two outliers. The more important process in setting the ε_{Nd} of Fe–Mn oxyhydroxides occurs *in situ*, within the pore waters.

4.7. A conceptual model relating the ε_{Nd} of authigenic phase to bottom water and detrital sediment

Although with our preferred leaching methods the contamination effects within the laboratory are very small or negligible, we find that the ε_{Nd} of GOA core-top leachates are systematically higher (more radiogenic) than bottom water (Fig. 3a). This is consistent with the findings of Abbott et al. (2015b) that pore water ε_{Nd} is more radiogenic than bottom water in the Northeast Pacific. Abbott et al. (2016) further suggested that authigenic phases exchange Nd with pore water and that detrital minerals could contribute to the formation of authigenic ε_{Nd} via their long-term influence on pore water ε_{Nd}. Other studies have also shown that mobilization of REEs from detrital sediments, including volcanic ash, during diagenesis is common, and that authigenic Fe–Mn oxyhydroxides and authigenic phosphates are sinks of pore water REEs (Palmer and Elderfield, 1985; Elderfield and Pagett, 1986; Elderfield and Sholkovitz, 1987; Toyoda and Tokonami, 1990; Rasmussen et al., 1998; Martin and Haley, 2000; Takebe, 2005; Caetano et al., 2009; Schacht et al., 2010; Soyol-Erdene and Huh, 2013; Takahashi et al., 2015; Chen et al., 2015). Here, we extend the study of Abbott et al. (2015b) and Abbott et al. (2016) to the basin scale and propose a conceptual model that relates the ε_{Nd} of authigenic phases to pore water, bottom water and detrital sediment (Fig. 9).

Traditionally a *diagenetic effect* in a paleoceanographic proxy is referred to as the alteration of an original signal by diagenesis post-burial. In this context previous studies have found minimal *diagenetic alternation* of authigenic ε_{Nd} during late diagenesis, such as the remobilization of Nd in Fe–Mn coatings and the recrystallization of carbonate and apatite after burial (Palmer and Elderfield, 1986; Murphy and Thomas, 2010). We agree that once authigenic phases are deeply buried their ε_{Nd} are unlikely to be subject to alteration during late diagenesis, mainly because of the extremely high Nd concentration in such phases relative to ambient pore water. However, ε_{Nd} is different from other paleoceanographic tracers in that it is carried in authigenic phases that are the *products* of sediment diagenesis (Froelich et al., 1979; Berner, 1980; Burdige and Gieskes, 1983; Canfield, 1989; Burdige, 1993, 2006; Poulton and Raiswell, 2002; van der Zee et al., 2003; Emerson and Hedges, 2003; Poulton and Canfield, 2005; Schulz and Zabel, 2006; Aller, 2014; Abbott et al., 2016), and therefore the original signal itself is a *diagenetic signal* (Palmer, 1985; Palmer and Elderfield, 1985; Toyoda and Tokonami, 1990; Abbott et al., 2016). We distinguish the *diagenetic formation* of authigenic ε_{Nd} in early diagenesis from its *diagenetic alteration* in late diagenesis.

Pore water can be considered as bottom water altered by sediment diagenesis (Schacht et al., 2010; Abbott et al., 2016). Once bottom water is buried through sedimentation, its ε_{Nd} starts to be modified by relatively slow release of Nd from sedimentary phases (Fig. 9). These sedimentary phases do not represent a uniform reservoir of Nd, rather, they include a spectrum of Nd-bearing phases with distinct reactivity and ε_{Nd} (Wilson et al., 2013; Abbott et al., 2016). Unlike our HH4 leaching experiments in which detrital sediment is only in contact with reagent for 30 min, detrital sediment may react with pore water on time scales of hundreds to thousands of years. This longer reaction time compensates for slow reaction kinetics, and allows bulk sediment to exert much greater influence on the Nd budget of pore water than it does in the laboratory leaches. Pore water ε_{Nd} depends on a balance of diffusive/advective exchange with bottom water and relatively slow release of Nd from sediments. As this process is setting the ε_{Nd} signature of pore water, authigenic Fe–Mn oxyhydroxides precipitate out of pore water and hence inherit its ε_{Nd} at the time and depth of precipitation (Fig. 9). Once these authigenic coatings are formed, their high concentration of Nd serve to buffer the pore water-bottom water Nd concentration gradient and hence benthic flux (Fig. 9) (Abbott et al., 2016).

If there were no benthic flux of Nd with a pore water ε_{Nd} signature, bottom water ε_{Nd} could reflect conservative mixing of the various water mass sources in the deep sea, assuming reversible scavenging is not important. The net benthic flux of Nd into bottom waters, however, makes ε_{Nd} in bottom waters non-conservative (Figs. 9 and 10), particularly in the Pacific (Jones et al., 2008; Horikawa et al., 2011). The degree of such modification of bottom water depends on the strength of the benthic source, the integrated exposure time of a water mass to such sources at the sea floor (Abbott et al., 2015b), and the reactivity and isotopic composition of the detrital sediments (Abbott et al., 2016).

Our finding that authigenic phases, and by implication pore water, have consistently higher ε_{Nd} values than GOA seawater agrees with this model, which explains observations that GOA seawater ε_{Nd} is more radiogenic than expected from conservative mixing between North Pacific Deep Water (NPDW) and North Pacific Intermediate Water (NPIW) at depths >500 m (Fig. 3a) (Haley et al., 2014; Abbott et al., 2015b). We suggest, perhaps in addition to reversible scavenging, the benthic flux of measured radiogenic authigenic ε_{Nd} explains such deviations.

Differences between core-top authigenic and bottom water ε_{Nd} similar to what we documented in the GOA are widespread in the Pacific and are observed in fish debris (Horikawa et al., 2011) and foraminifera (Vance et al., 2004; Ehlert et al., 2013; Molina-Kescher et al., 2014a). Extracted ε_{Nd} is almost always higher than bottom water in these cases, even becoming more radiogenic than the ε_{Nd} of operationally defined detrital residue (Ehlert et al., 2013). These results agree with the finding of Abbott et al. (2015b) and Abbott et al. (2016) that pore water ε_{Nd} is always more radiogenic than both bottom water and bulk sediment in the Northeast Pacific. According to our model and based on our GOA study, we attribute these differences to the long-term contribution of more reactive and more radiogenic (mostly volcanic) detrital components (Wilson et al., 2013) to pore water and thus to authigenic ε_{Nd}

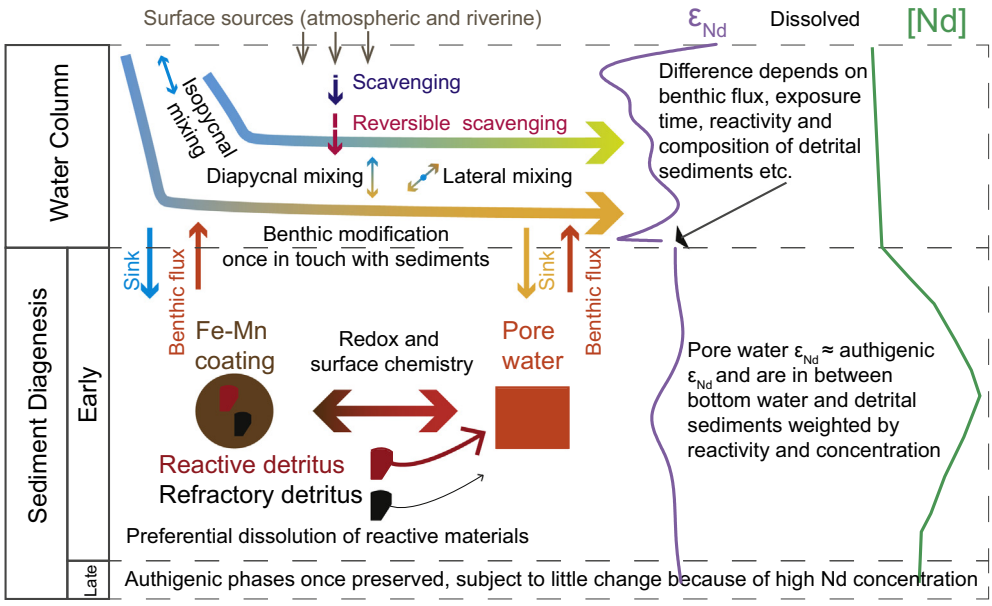

Fig. 9. A conceptual model describing the relationship of ε_{Nd} among authigenic phase, pore water, bottom water and detrital sediment. Water column and pore water ε_{Nd} and Nd concentration profiles are from the HH3000 site in Abbott et al. (2015b). The model is divided into water column, early diagenesis zone and late diagenesis zone. Bottom water is buried and becomes pore water, the isotopic compositions of which will be modified by the diagenesis of detrital sediments and authigenic phases. The detrital sediment comprises components of distinct reactivity and ε_{Nd}, which contribute to pore water Nd differentially. Fe–Mn oxyhydroxide forms in pore water and derives its ε_{Nd} at the time of formation. Once formed, Fe–Mn coatings become the most significant reactive Nd bearing phase in sediment as they have both high Nd concentration and reactivity. Interaction between Fe–Mn coatings and pore water supports a significant benthic flux of Nd, with pore water/authigenic ε_{Nd}. This flux modifies the bottom water ε_{Nd} and tends to shift bottom water ε_{Nd} toward pore water values. The difference between bottom water and pore water/authigenic ε_{Nd} depends on the magnitude of the benthic flux, the integrated time the bottom water is exposed to this flux (Abbott et al., 2015b), the reactivity and composition of detrital sediment . Along the circulation route bottom water ε_{Nd} derived from conservative water mass mixing is continuously modified by the benthic flux, while water-column processes like scavenging and reversible scavenging also affect deep-water ε_{Nd}. Water masses that are not directly in contact with sediment can still feel the benthic influence through lateral and diapycnal mixing. The sink term is not discussed in this study, but we assume it has the same ε_{Nd} as bottom water, while the benthic flux term has the ε_{Nd} of pore water. Once authigenic phases are preserved in the late diagenesis zone, their ε_{Nd} is insensitive to alternation because of high Nd concentration relative to the other solid and dissolved phases.

(Abbott et al., 2016). Even though they may be minor components of the total sediment, their high reactivity relative to bulk sediment increases their influence in pore water (Abbott et al., 2016). We distinguish such diagenetic contributions from laboratory detrital contamination (Fig. 8).

We propose that radiogenic benthic flux of Nd is widespread in the Pacific, and that this, rather than surface fluxes or internal cycling, explains the relatively radiogenic nature of deep Pacific seawater ε_{Nd} (Jones et al., 2008). We consider the benthic fluxes to be widespread in the deep sea, and thus separate from previous concepts of boundary exchange (e.g. Arsouze et al., 2009). Here we further show that the benthic flux concept of Abbott et al. (2015b) applies on the basin scale and is consistent with observations of relationships between deep water ε_{Nd} and water mass age. In the deep Pacific, the trend of deep water ε_{Nd} becoming more radiogenic from the Southern Ocean to the North Pacific is paralleled by the aging of water masses (Fig. 10a). We approximate the exposure time proposed in Abbott et al. (2015b) using water mass age based on radiocarbon (Khatiwala et al., 2012). With a box model, we can conduct a simply test of the sensitivity of deep water ε_{Nd} distribution to various magnitudes and isotope compositions of the benthic flux (Fig. 10b). Although this box model does not include sinks of Nd, as long as the isotopic composition of the sinks are close to the pore water or bottom water isotopic signature, the sinks would have little impact on the isotopic composition of Nd; the basic relationship of ε_{Nd} vs. age is robust to this model simplification. Model results suggest that, given the ranges of the magnitude (10–100 pmol cm^{-2} yr^{-1}) and the isotope composition (−6 to 0 ε_{Nd}) of the benthic flux that are consistent with observations of pore water (Haley and Klinkhammer, 2003; Schacht et al., 2010; Abbott et al., 2015a,b) and authigenic phases (this study, Vance et al., 2004; Horikawa et al., 2011; Ehlert et al., 2013; Molina-Kescher et al., 2014a), deep water ε_{Nd} distribution in the Pacific could indeed be reasonably captured (Fig. 10). Clearly, for anything beyond a first-order comparison, multi-component models and future pore water samplings on the abyssal plain would be necessary to improve the model-data fit. Nevertheless, this sensitivity test does indicate this is a reasonable hypothesis. In contrast, a pure conservative mixing model is inconsistent with the data (Fig. 10b) (Jones et al., 2008; Rempfer et al., 2011). Reversible scavenging is neglected here, so what is provided here likely overestimates the importance

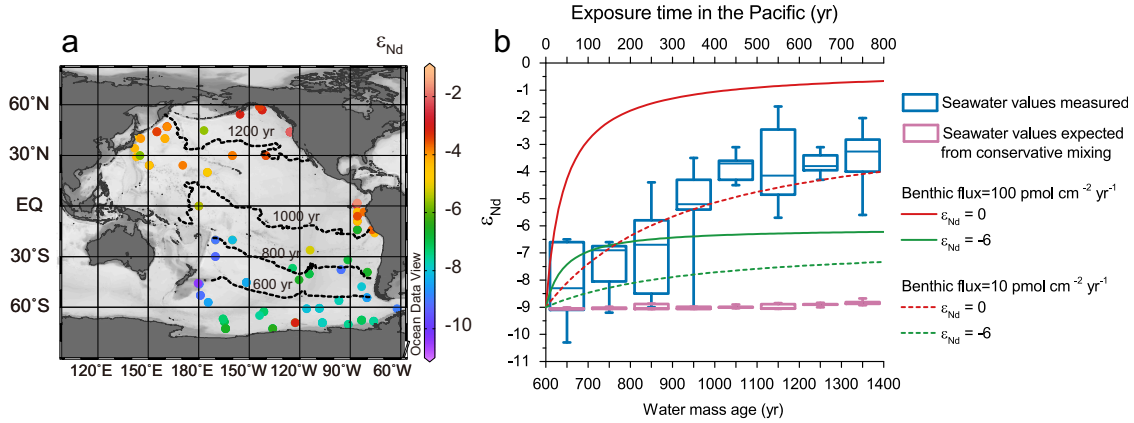

Fig. 10. The relationship between deep water ε_{Nd} and water mass age in the Pacific. (a) Contours of radiocarbon-based estimates of deep water mass age from Khatiwala et al. (2012) superimposed on the distribution of seawater ε_{Nd} over the depth range of 2500–4500 m. Data are from references in Lacan et al. (2012) and recent publications (Pahnke et al., 2012; Grasse et al., 2012; Grenier et al., 2013; Jeandel et al., 2013; Ehlert et al., 2013; Amakawa et al., 2013; Haley et al., 2014; Molina-Kescher et al., 2014b; Rickli et al., 2014; Basak et al., 2015; Abbott et al., 2015b). This figure is created using Ocean Data View (Schlitzer, 2014). (b) Deep water ε_{Nd} vs. age relationship (blue boxes, boxes span 25–75% of the data, whiskers note the entire range of values) compared to box model results (solid and dash lines). We assign a water mass age, based on the results from Khatiwala et al. (2012), to each seawater data point and bin the data into 100 yr intervals (blue boxes). The deep Pacific is treated as a single box, the circulation time scale of which is ~1000 yr (Khatiwala et al., 2012). We supply a uniform benthic flux to the box. The magnitude of the flux varies from 10 to 100 pmol cm^{-2} yr^{-1} and the isotope composition of the flux changes from −6 to 0. In this model the starting point of exposure to the benthic flux occurs when the southern sourced deep water enters the Pacific via the Deep Western Boundary Current east of New Zealand. This entering water mass has ε_{Nd} of −9 and Nd concentration of 22 pM (Molina-Kescher et al., 2014a,b) and the age of this water mass relative to surface waters is ~600 yrs (Khatiwala et al., 2012). Seawater ε_{Nd} expected from conservative water mass mixing only are also shown (purple boxes). We use the water mass decomposition product of Khatiwala et al. (2012), which gives the volumetric makeup of a deep ocean point computed using end members including Antarctic Bottom Water (AABW), North Atlantic Deep Water (NADW), Antarctic Intermediate Water (AAIW), North Pacific Intermediate Water (NPIW) and other surface water masses. The end member seawater ε_{Nd} data are chosen to be compatible with this set of water mass mixing ratios. All relevant data are presented in Table EA5 in the Electronic Annex. This model does not take into account reversible scavenging. (For interpretation of the references to colour in this figure legend, the reader is referred to the web version of this article.)

of benthic Nd flux; but the fact that this crude model, with its simplifications, can reasonably capture the distribution of ε_{Nd} in the entire deep Pacific to the first order suggests that benthic flux with pore water ε_{Nd} could be the dominant term in controlling the oceanic distribution of ε_{Nd}.

This conceptual model does not violate findings elsewhere that seawater ε_{Nd} could appear to behave conservatively and core-top authigenic and bottom water ε_{Nd} are similar. For example, in the North Atlantic, a combination of perhaps low benthic fluxes, short exposure times associated with rapid water mass ventilation, and weak detrital reactivity could lead to only slight benthic modification of bottom water ε_{Nd}, (Lambelet et al., 2016). On the other hand, Abbott et al. (2015b) has also shown that bottom water ε_{Nd} could approach pore water because of stronger benthic flux, longer exposure time, or similarity between water mass ε_{Nd} and detrital ε_{Nd}. This suggests that the "authenticity" of authigenic ε_{Nd} as a bottom water signal cannot be validated simply by showing *resemblance* between authigenic and bottom water ε_{Nd}.

4.8. Implication for ε_{Nd} in paleoceanography

Our hypothesis implies that the relevant question for the application of authigenic ε_{Nd} in paleoceanography is not whether authigenic phases and bottom water share similar ε_{Nd}, but what controls the variability of pore water ε_{Nd} in the past. The dynamic interactions between bottom water, pore water, authigenic phases and detrital sediments may seem to complicate the use of ε_{Nd}, but understanding these interactions is essential for recognizing proxy limitations and will likely also lead to new proxy opportunities. We suggest authigenic ε_{Nd} at a particular site of interest is derived from three processes (Fig. 9). Large-scale deep water formation and mixing determine the conservative mixing component of seawater ε_{Nd}. Along the circulation route this conservative component may be modified somewhat by reversible scavenging, but we suggested it is more significantly influenced by benthic fluxes that modify the water mass ε_{Nd} as a function of exposure time before arriving the studied site. Finally, this water mass signal is further modified locally during diagenetic cycling in which the authigenic and pore water ε_{Nd} are created *in situ*.

It is critical to understand the relative importance of these processes to interpret authigenic records in terms of paleoceanography. We suggest on the scale of the Pacific Ocean, local benthic modification is the most important term, for two main reasons: First, the time scale of local benthic process, i.e., early diagenesis, is generally much shorter than changes in water mass circulation (Froelich et al., 1979; Burdige, 2006), with a model estimate on the order of 0.2 yr for Nd (Arsouze et al., 2010). Second, the basin scale bottom boundary condition, i.e. core-top sediment composition and reactivity, is relatively invariant on

this time scale. In some other cases, such as in the modern Atlantic where the exposure time of bottom water masses to benthic fluxes is small relative to the mixing of different end-member water masses, the benthic flux "age" effect may not be dominant, but this does not mean it is absent or can be assumed to be irrelevant under different circulation regimes of the past.

The implications for the use of authigenic ε_{Nd} as a paleocirculation tracer are different under these two scenarios. In the first case, the deviation of authigenic from detrital ε_{Nd} could be used as a proxy for local ventilation rate, i.e. exposure time (Abbott et al., 2015b): fast circulation (low exposure time) may tend to decouple pore water and authigenic ε_{Nd} from the detrital values while leaving the water mass ε_{Nd} signal persistent in pore water and authigenic phases to certain degree; sluggish circulation would homogenize the ε_{Nd} of all these phases. The key challenge, however, is to separate this ventilation effect from any changes in local detrital composition and reactivity. For example, previous studies suggested authigenic ε_{Nd} could record events of changing sediment composition and were used as proxies for continental weathering, erosion and sediment provenance rather than circulation (Le Houedec et al., 2012; Cogez et al., 2015). Therefore, it is of fundamental importance to measure authigenic and detrital ε_{Nd} concurrently. In the second case, authigenic ε_{Nd} might be used as a quasi-conservative water mass tracer much as it is widely adopted in modern literature, but even in this case it is key to recognize the water mass ε_{Nd} is not simply the result of conservative water mass mixing but the benthic modification along the circulation route needs to be considered, i.e. authigenic ε_{Nd} could be still different from the values expected of conservative mixing. While these are end member cases, in more general situations aspects from both cases could exist. Therefore, understanding the role of sediment-water interaction in the oceanic and diagenetic cycles of Nd is critical in both modern and paleoceanographic applications.

5. CONCLUSION

We developed a robust leaching method to extract authigenic ε_{Nd} from bulk sediment and applied it to a set of core-top samples in the GOA. We show that in our experiments one dominant phase is extracted during leaching, and by comparing leachates to selected detrital and authigenic end members using major and trace element signatures, we conclude that the extracted phase is Fe–Mn oxyhydroxide. Detrital contamination of leachate Nd, estimated using kinetic mineral dissolution rate, leaching fresh and marine volcanic ash samples and ε_{Nd} -$^{87}Sr/^{86}Sr$ mass balance calculations, is typically on the order of 1% and does not bias the authigenic ε_{Nd} signal beyond analytical uncertainty; thus, our leaching method accurately reflects the composition of authigenic Fe–Mn oxyhydroxide.

The ε_{Nd} of GOA core-top leachates are consistently higher than bottom water, even though carbonate-corrected $^{87}Sr/^{86}Sr$ of leachates are very close to modern seawater at water depths >3000 m. These observations are reconciled if the authigenic phases record the isotopic values of pore water rather than bottom water.

We propose a conceptual model to describe the relationship among the leached authigenic phase, pore water, bottom water and detrital sediment, which includes differential reactivity of detrital components, the ε_{Nd} signature of these components, benthic fluxes of Nd, and the time that bottom waters are in contact with the sea floor. This model suggests that on long circulation timescales ε_{Nd} is a non-conservative water mass tracer. We show that this conceptual model can be applied on the Pacific basin scale by simulating the relationship between water mass age and water mass ε_{Nd} in the deep Pacific. In general, different scenarios of parameter combination (benthic flux, detrital composition and reactivity, exposure time etc.) under this new framework can accommodate observations that seawater ε_{Nd} appears to behave conservatively in some regions (for example, the modern Atlantic where benthic exposure times are small relative to the mixing of different water mass end members) and that core-top authigenic and bottom water ε_{Nd} are similar.

Our finding that authigenic ε_{Nd} records pore water rather than bottom water signatures requires a new framework for the use of ε_{Nd} as a circulation tracer in paleoceanography. In particular, we recommend that authigenic and detrital ε_{Nd} should be measured concurrently and the deviation of authigenic from detrital ε_{Nd} can be used as a proxy for local bottom water ventilation rate, if local benthic modification is the dominant factor controlling the formation of authigenic ε_{Nd} and detrital composition and reactivity are time invariant. On the other hand, if the local benthic process is of secondary importance, the traditional quasi-conservative trace approach might be appropriate, bearing in mind that even in this case the water mass ε_{Nd} signal recorded in authigenic phases may not necessarily be the same as expected from conservative water mass mixing, because of the benthic modification along the circulation route.

ACKNOWLEDGEMENTS

We thank David Graham for donating the Mount St. Helens ash samples. Jesse Muratli was instrumental at the early stage of data collection of this project and offered lab assistance. Andy Ungerer from the W.M. Keck Collaboratory for Plasma Mass Spectrometry at Oregon State University provided technical supports for the quadrupole ICP-MS and ICP-OES measurements. Discussion with April Abbott improved our understanding of pore water Nd geochemistry. We also appreciate the help from Mysti Weber and Maziet Cheseby in sampling and interpreting smear slide results at the Marine Geology Repository of Oregon State University. We gratefully acknowledge Editor Tina van de Flierdt, David Wilson and two anonymous reviewers for thorough and thoughtful comments that significantly improved our manuscript. The U.S. National Science Foundation (NSF), Division of Ocean Sciences supported this research through Grant No. OCE-1357529.

APPENDIX A. SUPPLEMENTARY DATA

Supplementary data associated with this article can be found, in the online version, at http://dx.doi.org/10.1016/j.gca.2016.08.005.

REFERENCES

Abbott A. N., Haley B. A. and McManus J. (2015a) Bottoms up: Sedimentary control of the deep North Pacific Ocean's εNd signature. *Geology* **43**, 1035.

Abbott A. N., Haley B. A., McManus J. and Reimers C. E. (2015b) The sedimentary flux of dissolved rare earth elements to the ocean. *Geochim. Cosmochim. Acta* **154**, 186–200.

Abbott A. N., Haley B. A. and McManus J. (2016) The impact of sedimentary coatings on the diagenetic Nd flux. *Earth Planet. Sci. Lett.* **449**, 217–227.

Akagi T., Fu F., Hongo Y. and Takahashi K. (2011) Composition of rare earth elements in settling particles collected in the highly productive North Pacific Ocean and Bering Sea: Implications for siliceous-matter dissolution kinetics and formation of two REE-enriched phases. *Geochim. Cosmochim. Acta* **75**, 4857–4876.

Aller R. C. (2014) 8.11 – Sedimentary diagenesis, depositional environments, and benthic fluxes A2 – Holland, Heinrich D. In *Treatise on Geochemistry* (ed. K. K. Turekian), second ed. Elsevier, Oxford, pp. 293–334.

Amakawa H., Tazoe H., Obata H., Gamo T., Sano Y. and Chuan-Chou S. (2013) Neodymium isotopic composition and concentration in the Southwest Pacific Ocean. *Geochem. J.* **47**, 409–422.

Arsouze T., Dutay J.-C., Lacan F. and Jeandel C. (2009) Reconstructing the Nd oceanic cycle using a coupled dynamical – biogeochemical model. *Biogeosciences* **6**, 2829–2846.

Arsouze T., Treguier A. M., Peronne S., Dutay J.-C., Lacan F. and Jeandel C. (2010) Modeling the Nd isotopic composition in the North Atlantic basin using an eddy-permitting model. *Ocean Sci* **6**, 789–797.

Bacon M. P. and Anderson R. F. (1982) Distribution of thorium isotopes between dissolved and particulate forms in the deep sea. *J. Geophys. Res. Oceans* **87**, 2045–2056.

Bandstra J. Z. and Brantley S. L. (2008) Data fitting techniques with applications to mineral dissolution kinetics. In *Kinetics of Water–Rock Interaction* (eds. S. L. Brantley, J. D. Kubicki and A. F. White). Springer, New York, pp. 211–257.

Basak C., Pahnke K., Frank M., Lamy F. and Gersonde R. (2015) Neodymium isotopic characterization of Ross Sea Bottom Water and its advection through the southern South Pacific. *Earth Planet. Sci. Lett.* **419**, 211–221.

Bau M., Tepe N. and Mohwinkel D. (2013) Siderophore-promoted transfer of rare earth elements and iron from volcanic ash into glacial meltwater, river and ocean water. *Earth Planet. Sci. Lett.* **364**, 30–36.

Bayon G., German C. R., Boella R. M., Milton J. A., Taylor R. N. and Nesbitt R. W. (2002) An improved method for extracting marine sediment fractions and its application to Sr and Nd isotopic analysis. *Chem. Geol.* **187**, 179–199.

Bayon G., German C. R., Burton K. W., Nesbitt R. W. and Rogers N. (2004) Sedimentary Fe–Mn oxyhydroxides as paleoceanographic archives and the role of aeolian flux in regulating oceanic dissolved REE. *Earth Planet. Sci. Lett.* **224**, 477–492.

Bayon G., Toucanne S., Skonieczny C., André L., Bermell S., Cheron S., Dennielou B., Etoubleau J., Freslon N., Gauchery T., Germain Y., Jorry S. J., Ménot G., Monin L., Ponzevera E., Rouget M.-L., Tachikawa K. and Barrat J. A. (2015) Rare earth elements and neodymium isotopes in world river sediments revisited. *Geochim. Cosmochim. Acta* **170**, 17–38.

Berner R. A. (1980) *Early Diagenesis: A Theoretical Approach*. Princeton University Press.

Bertram C. J. and Elderfield H. (1993) The geochemical balance of the rare earth elements and neodymium isotopes in the oceans. *Geochim. Cosmochim. Acta* **57**, 1957–1986.

Blaser P., Lippold J., Gutjahr M., Frank N., Link J. M. and Frank M. (2016) Extracting foraminiferal seawater Nd isotope signatures from bulk deep sea sediment by chemical leaching. *Chem. Geol.* **439**, 189–204.

Böhm E., Lippold J., Gutjahr M., Frank M., Blaser P., Antz B., Fohlmeister J., Frank N., Andersen M. B. and Deininger M. (2015) Strong and deep Atlantic meridional overturning circulation during the last glacial cycle. *Nature* **517**, 73–76.

Brantley S. L. (2008) Kinetics of mineral dissolution. In *Kinetics of Water–Rock Interaction* (eds. S. L. Brantley, J. D. Kubicki and A. F. White). Springer, New York, pp. 151–210.

Burdige D. J. (1993) The biogeochemistry of manganese and iron reduction in marine sediments. *Earth-Sci. Rev.* **35**, 249–284.

Burdige D. J. (2006) *Geochemistry of Marine Sediments*. Princeton University Press.

Burdige D. J. and Gieskes J. M. (1983) A pore water/solid phase diagenetic model for manganese in marine sediments. *Am. J. Sci.* **283**, 29–47.

Byrne R. H. and Kim K.-H. (1990) Rare earth element scavenging in seawater. *Geochim. Cosmochim. Acta* **54**, 2645–2656.

Caetano M., Prego R., Vale C., de Pablo H. and Marmolejo-Rodríguez J. (2009) Record of diagenesis of rare earth elements and other metals in a transitional sedimentary environment. *Mar. Chem.* **116**, 36–46.

Canfield D. E. (1989) Reactive iron in marine sediments. *Geochim. Cosmochim. Acta* **53**, 619–632.

Cao L. Q. and Arculus R. J. (1995) Data report: geochemistry of volcanic ashes recovered from Hole 887A. In *Proc. ODP, Sci. Results* (eds. D. K. Rea, I. A. Basov, D. W. Scholl and J. F. Allan). Ocean Drilling Program, College Station, TX, pp. 661–669.

Chen J., Algeo T. J., Zhao L., Chen Z.-Q., Cao L., Zhang L. and Li Y. (2015) Diagenetic uptake of rare earth elements by bioapatite, with an example from Lower Triassic conodonts of South China. *Earth-Sci. Rev.* **149**, 181–202.

Cogez A., Meynadier L., Allègre C., Limmois D., Herman F. and Gaillardet J. (2015) Constraints on the role of tectonic and climate on erosion revealed by two time series analysis of marine cores around New Zealand. *Earth Planet. Sci. Lett.* **410**, 174–185.

Davies M. H., Mix A. C., Stoner J. S., Addison J. A., Jaeger J., Finney B. and Wiest J. (2011) The deglacial transition on the southeastern Alaska Margin: meltwater input, sea level rise, marine productivity, and sedimentary anoxia. *Paleoceanography* **26**, PA2223.

Davies-Walczak M., Mix A. C., Stoner J. S., Southon J. R., Cheseby M. and Xuan C. (2014) Late Glacial to Holocene radiocarbon constraints on North Pacific Intermediate Water ventilation and deglacial atmospheric CO_2 sources. *Earth Planet. Sci. Lett.* **397**, 57–66.

Ehlert C., Grasse P. and Frank M. (2013) Changes in silicate utilisation and upwelling intensity off Peru since the Last Glacial Maximum – insights from silicon and neodymium isotopes. *Quat. Sci. Rev.* **72**, 18–35.

Elderfield H. and Gieskes J. M. (1982) Sr isotopes in interstitial waters of marine sediments from Deep Sea Drilling Project cores. *Nature* **300**, 493–497.

Elderfield H. and Pagett R. (1986) Analytical chemistry in marine sciences rare earth elements in ichthyoliths: variations with redox conditions and depositional environment. *Sci. Total Environ.* **49**, 175–197.

Elderfield H. and Sholkovitz E. R. (1987) Rare earth elements in the pore waters of reducing nearshore sediments. *Earth Planet. Sci. Lett.* **82**, 280–288.

Elmore A. C., Piotrowski A. M., Wright J. D. and Scrivner A. E. (2011) Testing the extraction of past seawater Nd isotopic

composition from North Atlantic deep sea sediments and foraminifera. *Geochem. Geophys. Geosystems* **12**, Q09008.

Emerson S. and Hedges J. (2003) Sediment diagenesis and benthic flux. *Treatise Geochem.* **6**, 625.

Farmer G. L., Ayuso R. and Plafker G. (1993) A Coast Mountains provenance for the Valdez and Orca groups, southern Alaska, based on Nd, Sr, and Pb isotopic evidence. *Earth Planet. Sci. Lett.* **116**, 9–21.

van de Flierdt T. (2003) The Nd, Hf, and Pb isotopic composition of ferromanganese crusts and their paleoceanographic implications., Diss., Naturwissenschaften ETH Zürich, Nr. 15188, 2003.

Frank M. (2002) Radiogenic isotopes: Tracers of past ocean circulation and erosional input. *Rev. Geophys.* **40**, 1001.

Freslon N., Bayon G., Toucanne S., Bermell S., Bollinger C., Chéron S., Etoubleau J., Germain Y., Khripounoff A., Ponzevera E. and Rouget M.-L. (2014) Rare earth elements and neodymium isotopes in sedimentary organic matter. *Geochim. Cosmochim. Acta* **140**, 177–198.

Froelich P. N., Klinkhammer G. P., Bender M. L., Luedtke N. A., Heath G. R., Cullen D., Dauphin P., Hammond D., Hartman B. and Maynard V. (1979) Early oxidation of organic matter in pelagic sediments of the eastern equatorial Atlantic: suboxic diagenesis. *Geochim. Cosmochim. Acta* **43**, 1075–1090.

Garcia H. E., Locarnini R. A., Boyer T. P., Antonov J. I., Baranova O. K., Zweng M. M., Reagan J. R. and Johnson D. R. (2014) Dissolved oxygen, apparent oxygen utilization, and oxygen saturation. In *World Ocean Atlas 2013* (eds. S. Levitus and A. Mishonov). NOAA Atlas NESDIS.

German C. R. and Elderfield H. (1989) Rare earth elements in Saanich Inlet, British Columbia, a seasonally anoxic basin. *Geochim. Cosmochim. Acta* **53**, 2561–2571.

Goldstein S. L. and Hemming S. R. (2003) Long-lived isotopic tracers in oceanography, paleoceanography, and ice-sheet dynamics. In *Treatise on Geochemistry* (eds. H. D. Holland and K. K. Turekian). Pergamon, Oxford, pp. 453–489.

Goldstein S. L., Onions R. K. and Hamilton P. J. (1984) A Sm–Nd isotopic study of atmospheric dusts and particulates from major river systems. *Earth Planet. Sci. Lett.* **70**, 221–236.

Gourlan A. T., Meynadier L. and Allègre C. J. (2008) Tectonically driven changes in the Indian Ocean circulation over the last 25 Ma: neodymium isotope evidence. *Earth Planet. Sci. Lett.* **267**, 353–364.

Gourlan A. T., Meynadier L., Allègre C. J., Tapponnier P., Birck J.-L. and Joron J.-L. (2010) Northern Hemisphere climate control of the Bengali rivers discharge during the past 4 Ma. *Quat. Sci. Rev.* **29**, 2484–2498.

Grasse P., Stichel T., Stumpf R., Stramma L. and Frank M. (2012) The distribution of neodymium isotopes and concentrations in the Eastern Equatorial Pacific: water mass advection versus particle exchange. *Earth Planet. Sci. Lett.* **353–354**, 198–207.

Grenier M., Jeandel C., Lacan F., Vance D., Venchiarutti C., Cros A. and Cravatte S. (2013) From the subtropics to the central equatorial Pacific Ocean: neodymium isotopic composition and rare earth element concentration variations. *J. Geophys. Res. Oceans* **118**, 592–618.

Gulick S. P. S., Jaeger J. M., Mix A. C., Asahi H., Bahlburg H., Belanger C. L., Berbel G. B. B., Childress L., Cowan E., Drab L., Forwick M., Fukumura A., Ge S., Gupta S., Kioka A., Konno S., LeVay L. J., März C., Matsuzaki K. M., McClymont E. L., Moy C., Müller J., Nakamura A., Ojima T., Ribeiro F. R., Ridgway K. D., Romero O. E., Slagle A. L., Stoner J. S., St-Onge G., Suto I., Walczak M. D., Worthington L. L., Bailey I., Enkelmann E., Reece R. and Swartz J. M. (2015) Mid-Pleistocene climate transition drives net mass loss from rapidly uplifting St. Elias Mountains, Alaska. *Proc. Natl. Acad. Sci.* **112**, 15042–15047.

Gutjahr M., Frank M., Stirling C. H., Klemm V., van de Flierdt T. and Halliday A. N. (2007) Reliable extraction of a deepwater trace metal isotope signal from Fe–Mn oxyhydroxide coatings of marine sediments. *Chem. Geol.* **242**, 351–370.

Gutjahr M., Frank M., Stirling C. H., Keigwin L. D. and Halliday A. N. (2008) Tracing the Nd isotope evolution of North Atlantic Deep and Intermediate Waters in the western North Atlantic since the Last Glacial Maximum from Blake Ridge sediments. *Earth Planet. Sci. Lett.* **266**, 61–77.

Gutjahr M., Hoogakker B. A. A., Frank M. and McCave I. N. (2010) Changes in North Atlantic Deep Water strength and bottom water masses during Marine Isotope Stage 3 (45–35 kaBP). *Quat. Sci. Rev.* **29**, 2451–2461.

Haley B. A. and Klinkhammer G. P. (2003) Complete separation of rare earth elements from small volume seawater samples by automated ion chromatography: method development and application to benthic flux. *Mar. Chem.* **82**, 197–220.

Haley B. A., Klinkhammer G. P. and McManus J. (2004) Rare earth elements in pore waters of marine sediments. *Geochim. Cosmochim. Acta* **68**, 1265–1279.

Haley B. A., Klinkhammer G. P. and Mix A. C. (2005) Revisiting the rare earth elements in foraminiferal tests. *Earth Planet. Sci. Lett.* **239**, 79–97.

Haley B. A., Frank M., Hathorne E. and Pisias N. (2014) Biogeochemical implications from dissolved rare earth element and Nd isotope distributions in the Gulf of Alaska. *Geochim. Cosmochim. Acta* **126**, 455–474.

Halliday A. N., Fallick A. E., Dickin A. P., Mackenzie A. B., Stephens W. E. and Hildreth W. (1983) The isotopic and chemical evolution of Mount St. Helens. *Earth Planet. Sci. Lett.* **63**, 241–256.

Hein J. R. and Koschinsky A. (2014) Deep-ocean ferromanganese crusts and nodules. In *Treatise on Geochemistry* (eds. H. D. Holland and K. K. Turekian), second ed. Elsevier, Oxford, pp. 273–291.

Hildreth W. and Fierstein J. (2012) The Novarupta-Katmai Eruption of 1912—Largest Eruption of the Twentieth Century: Centennial Perspective, U.S. Geological Survey Professional Paper 1791.

Horikawa K., Asahara Y., Yamamoto K. and Okazaki Y. (2010) Intermediate water formation in the Bering Sea during glacial periods: evidence from neodymium isotope ratios. *Geology* **38**, 435–438.

Horikawa K., Martin E. E., Asahara Y. and Sagawa T. (2011) Limits on conservative behavior of Nd isotopes in seawater assessed from analysis of fish teeth from Pacific core tops. *Earth Planet. Sci. Lett.* **310**, 119–130.

Huang K.-F., Oppo D. W. and Curry W. B. (2014) Decreased influence of Antarctic intermediate water in the tropical Atlantic during North Atlantic cold events. *Earth Planet. Sci. Lett.* **389**, 200–208.

Jacobsen S. B. and Wasserburg G. J. (1980) Sm–Nd isotopic evolution of chondrites. *Earth Planet. Sci. Lett.* **50**, 139–155.

Jeandel C., Delattre H., Grenier M., Pradoux C. and Lacan F. (2013) Rare earth element concentrations and Nd isotopes in the Southeast Pacific Ocean. *Geochem. Geophys. Geosystems* **14**, 328–341.

Jaeger J. M., Gulick S. P. S. and LeVay L. J. (2014) Expedition 341 scientists. In *Proc. IODP*, 341. Integrated Ocean Drilling Program, College Station, TX.

Jeandel C. and Oelkers E. H. (2015) The influence of terrigenous particulate material dissolution on ocean chemistry and global element cycles. *Chem. Geol.* **395**, 50–66.

Johannesson K. H. and Burdige D. J. (2007) Balancing the global oceanic neodymium budget: evaluating the role of groundwater. *Earth Planet. Sci. Lett.* **253**, 129–142.

Jones C. E., Halliday A. N., Rea D. K. and Owen R. M. (1994) Neodymium isotopic variations in North Pacific modern silicate sediment and the insignificance of detrital REE contributions to seawater. *Earth Planet. Sci. Lett.* **127**, 55–66.

Jones K. M., Khatiwala S. P., Goldstein S. L., Hemming S. R. and van de Flierdt T. (2008) Modeling the distribution of Nd isotopes in the oceans using an ocean general circulation model. *Earth Planet. Sci. Lett.* **272**, 610–619.

Jones M. T., Pearce C. R., Jeandel C., Gislason S. R., Eiriksdottir E. S., Mavromatis V. and Oelkers E. H. (2012) Riverine particulate material dissolution as a significant flux of strontium to the oceans. *Earth Planet. Sci. Lett.* **355–356**, 51–59.

Kawabe M. and Fujio S. (2010) Pacific Ocean circulation based on observation. *J. Oceanogr.* **66**, 389–403.

Kelemen P. B., Yogodzinski G. M. and Scholl D. W. (2004) Along-strike variation in the Aleutian island arc: genesis of high Mg# andesite and implications for continental crust. In *Inside the Subduction Factory* (ed. J. Eiler). American Geophysical Union, pp. 223–276.

Kelemen P. B., Hanghøj K. and Greene A. R. (2014) One view of the geochemistry of subduction-related magmatic arcs, with an emphasis on primitive andesite and lower crust. In *Treatise on Geochemistry* (eds. H. D. Holland and K. K. Turekian), second ed. Elsevier, Oxford, pp. 749–806.

Khatiwala S., Primeau F. and Holzer M. (2012) Ventilation of the deep ocean constrained with tracer observations and implications for radiocarbon estimates of ideal mean age. *Earth Planet. Sci. Lett.* **325–326**, 116–125.

Kraft S., Frank M., Hathorne E. C. and Weldeab S. (2013) Assessment of seawater Nd isotope signatures extracted from foraminiferal shells and authigenic phases of Gulf of Guinea sediments. *Geochim. Cosmochim. Acta* **121**, 414–435.

Lacan F. and Jeandel C. (2005) Neodymium isotopes as a new tool for quantifying exchange fluxes at the continent–ocean interface. *Earth Planet. Sci. Lett.* **232**, 245–257.

Lacan F., Tachikawa K. and Jeandel C. (2012) Neodymium isotopic composition of the oceans: a compilation of seawater data. *Chem. Geol.* **300–301**, 177–184.

Lambelet M., van de Flierdt T., Crocket K., Rehkämper M., Kreissig K., Coles B., Rijkenberg M. J. A., Gerringa L. J. A., de Baar H. J. W. and Steinfeldt R. (2016) Neodymium isotopic composition and concentration in the western North Atlantic Ocean: results from the GEOTRACES GA02 section. *Geochim. Cosmochim. Acta* **177**, 1–29.

Le Houedec S., Meynadier L. and Allègre C. J. (2012) Nd isotope systematics on ODP Sites 756 and 762 sediments reveal major volcanic, oceanic and climatic changes in South Indian Ocean over the last 35 Ma. *Earth Planet. Sci. Lett.* **327–328**, 29–38.

Martin E. E. and Haley B. A. (2000) Fossil fish teeth as proxies for seawater Sr and Nd isotopes. *Geochim. Cosmochim. Acta* **64**, 835–847.

Martin E. E., Macdougall J. D., Herbert T. D., Paytan A. and Kastner M. (1995) Strontium and neodymium isotopic analyses of marine barite separates. *Geochim. Cosmochim. Acta* **59**, 1353–1361.

Martin E. E., Blair S. W., Kamenov G. D., Scher H. D., Bourbon E., Basak C. and Newkirk D. N. (2010) Extraction of Nd isotopes from bulk deep sea sediments for paleoceanographic studies on Cenozoic time scales. *Chem. Geol.* **269**, 414–431.

McLennan S. M. (1989) Rare earth elements in sedimentary rocks; influence of provenance and sedimentary processes. *Rev. Mineral. Geochem.* **21**, 169–200.

McLennan S. M. (2001) Relationships between the trace element composition of sedimentary rocks and upper continental crust. *Geochem. Geophys. Geosystems* **2**, 1021.

McLennan S. M., Hemming S., McDaniel D. K. and Hanson G. N. (1993) Geochemical approaches to sedimentation, provenance, and tectonics. *Geol. Soc. Am. Spec. Pap.* **284**, 21–40.

Mokadem F., Parkinson I. J., Hathorne E. C., Anand P., Allen J. T. and Burton K. W. (2015) High-precision radiogenic strontium isotope measurements of the modern and glacial ocean: limits on glacial–interglacial variations in continental weathering. *Earth Planet. Sci. Lett.* **415**, 111–120.

Molina-Kescher M., Frank M. and Hathorne E. (2014a) Nd and Sr isotope compositions of different phases of surface sediments in the South Pacific: extraction of seawater signatures, boundary exchange, and detrital/dust provenance. *Geochem. Geophys. Geosystems* **15**, 3502–3520.

Molina-Kescher M., Frank M. and Hathorne E. (2014b) South Pacific dissolved Nd isotope compositions and rare earth element distributions: water mass mixing versus biogeochemical cycling. *Geochim. Cosmochim. Acta* **127**, 171–189.

Muratli J. M., McManus J., Mix A. and Chase Z. (2012) Dissolution of fluoride complexes following microwave-assisted hydrofluoric acid digestion of marine sediments. *Talanta* **89**, 195–200.

Murphy D. P. and Thomas D. J. (2010) The negligible role of intermediate water circulation in stadial–interstadial oxygenation variations along the southern California margin: evidence from Nd isotopes. *Quat. Sci. Rev.* **29**, 2442–2450.

Nokleberg W. J., Parfenov L. M., Monger J. W. H., Norton I. O., Khanchuk A. I., Stone D. B., Scotese C. R., Scholl D. W. and Fujita K. (2000) *Phanerozoic tectonic evolution of the circum-north Pacific*. U.S. Geological Survey.

O'Nions R. K., Carter S. R., Evensen N. M. and Hamilton P. J. (1979) Geochemical and cosmochemical applications of Nd isotope analysis. *Annu. Rev. Earth Planet. Sci.* **7**, 11–38.

Pahnke K., van de Flierdt T., Jones K. M., Lambelet M., Hemming S. R. and Goldstein S. L. (2012) GEOTRACES intercalibration of neodymium isotopes and rare earth element concentrations in seawater and suspended particles. Part 2: systematic tests and baseline profiles. *Limnol. Oceanogr. Methods* **10**, 252–269.

Palmer M. R. (1985) Rare earth elements in foraminifera tests. *Earth Planet. Sci. Lett.* **73**, 285–298.

Palmer M. R. and Elderfield H. (1985) Variations in the Nd isotopic composition of foraminifera from Atlantic Ocean sediments. *Earth Planet. Sci. Lett.* **73**, 299–305.

Palmer M. R. and Elderfield H. (1986) Rare earth elements and neodymium isotopes in ferromanganese oxide coatings of Cenozoic foraminifera from the Atlantic Ocean*. *Geochim. Cosmochim. Acta* **50**, 409–417.

Piotrowski A. M., Goldstein S. L., Hemming S. R. and Fairbanks R. G. (2004) Intensification and variability of ocean thermohaline circulation through the last deglaciation. *Earth Planet. Sci. Lett.* **225**, 205–220.

Plank T. (2014) The chemical composition of subducting sediments. In *Treatise on Geochemistry* (eds. H. D. Holland and K. K. Turekian), second ed. Elsevier, Oxford, pp. 607–629.

Plank T. and Langmuir C. H. (1998) The chemical composition of subducting sediment and its consequences for the crust and mantle. *Chem. Geol.* **145**, 325–394.

Poulton S. W. and Canfield D. E. (2005) Development of a sequential extraction procedure for iron: implications for iron partitioning in continentally derived particulates. *Chem. Geol.* **214**, 209–221.

Poulton S. W. and Raiswell R. (2002) The low-temperature geochemical cycle of iron: from continental fluxes to marine sediment deposition. *Am. J. Sci.* **302**, 774–805.

Poulton S. W. and Raiswell R. (2005) Chemical and physical characteristics of iron oxides in riverine and glacial meltwater sediments. *Chem. Geol.* **218**, 203–221.

Praetorius S. K., Mix A. C., Walczak M. H., Wolhowe M. D., Addison J. A. and Prahl F. G. (2015) North Pacific deglacial hypoxic events linked to abrupt ocean warming. *Nature*.

Pratt R. M., Scheidegger K. F. and Kulm L. D. (1973) Volcanic ash from DSDP Site 178, Gulf of Alaska. In *Initial Reports of the Deep Sea Drilling Project* (eds. L. D. Kulm and R. von Huene). U.S. Govt. Printing Office, Washington, D.C., pp. 833–834.

Rasmussen B., Buick R. and Taylor W. R. (1998) Removal of oceanic REE by authigenic precipitation of phosphatic minerals. *Earth Planet. Sci. Lett.* **164**, 135–149.

Rempfer J., Stocker T. F., Joos F., Dutay J.-C. and Siddall M. (2011) Modelling Nd-isotopes with a coarse resolution ocean circulation model: sensitivities to model parameters and source/sink distributions. *Geochim. Cosmochim. Acta* **75**, 5927–5950.

Rickli J., Gutjahr M., Vance D., Fischer-Gödde M., Hillenbrand C.-D. and Kuhn G. (2014) Neodymium and hafnium boundary contributions to seawater along the West Antarctic continental margin. *Earth Planet. Sci. Lett.* **394**, 99–110.

Roberts N. L. and Piotrowski A. M. (2015) Radiogenic Nd isotope labeling of the northern NE Atlantic during MIS 2. *Earth Planet. Sci. Lett.* **423**, 125–133.

Roberts N. L., Piotrowski A. M., Elderfield H., Eglinton T. I. and Lomas M. W. (2012) Rare earth element association with foraminifera. *Geochim. Cosmochim. Acta* **94**, 57–71.

Rousseau T. C. C., Sonke J. E., Chmeleff J., van Beek P., Souhaut M., Boaventura G., Seyler P. and Jeandel C. (2015) Rapid neodymium release to marine waters from lithogenic sediments in the Amazon estuary. *Nat. Commun.* **6**, 7592.

Rudnick R. L. and Gao S. (2014) Composition of the continental crust. In *Treatise on Geochemistry* (eds. H. D. Holland and K. K. Turekian), second ed. Elsevier, Oxford, pp. 1–51.

Rutberg R. L., Hemming S. R. and Goldstein S. L. (2000) Reduced North Atlantic Deep Water flux to the glacial Southern Ocean inferred from neodymium isotope ratios. *Nature* **405**, 935–938.

Samson S. D., McClelland W. C., Patchett P. J., Gehrels G. E. and Anderson R. G. (1989) Evidence from neodymium isotopes for mantle contributions to Phanerozoic crustal genesis in the Canadian Cordillera. *Nature* **337**, 705–709.

Samson S. D., Patchett P. J., Gehrels G. E. and Anderson R. G. (1990) Nd and Sr isotopic characterization of the wrangellia terrane and implications for crustal growth of the Canadian Cordillera. *J. Geol.* **98**, 749–762.

Samson S. D., Patchett P. J., McClelland W. C. and Gehrels G. E. (1991a) Nd and Sr isotopic constraints on the petrogenesis of the west side of the northern Coast Mountains batholith, Alaskan and Canadian Cordillera. *Can. J. Earth Sci.* **28**, 939–946.

Samson S. D., Patchett P. J., McClelland W. C. and Gehrels G. E. (1991b) Nd isotopic characterization of metamorphic rocks in the Coast Mountains, Alaskan and Canadian Cordillera: ancient crust bounded by juvenile terranes. *Tectonics* **10**, 770–780.

Sarmiento J. L. and Gruber N. (2013) *Ocean Biogeochemical Dynamics*. Princeton University Press.

Schacht U., Wallmann K. and Kutterolf S. (2010) The influence of volcanic ash alteration on the REE composition of marine pore waters. *J. Geochem. Explor.* **106**, 176–187.

Scheidegger K. F. and Kulm L. D. (1975) Late Cenozoic volcanism in the Aleutian Arc: information from ash layers in the northeastern Gulf of Alaska. *Geol. Soc. Am. Bull.* **86**, 1407–1412.

Scheidegger K., Corliss J., Jezek P. and Ninkovich D. (1980) Compositions of deep-sea ash layers derived from North Pacific Volcanic Arcs – variations in time and space. *J. Volcanol. Geotherm. Res.* **7**, 107–137.

Schijf J., Christenson E. A. and Byrne R. H. (2015) YREE scavenging in seawater: A new look at an old model. *Mar. Chem.* **177**(Part 3), 460–471.

Schlitzer R. (2014) Ocean data view Available at: http://odv.awi.de.

Schulz H. D. and Zabel M. (2006) *Marine Geochemistry*. Springer Science & Business Media.

Shaw H. F. and Wasserburg G. J. (1985) Sm–Nd in marine carbonates and phosphates: implications for Nd isotopes in seawater and crustal ages. *Geochim. Cosmochim. Acta* **49**, 503–518.

Sholkovitz E. R. and Elderfield H. (1988) Cycling of dissolved rare earth elements in Chesapeake Bay. *Glob. Biogeochem. Cycles* **2**, 157–176.

Sholkovitz E. R., Landing W. M. and Lewis B. L. (1994) Ocean particle chemistry: the fractionation of rare earth elements between suspended particles and seawater. *Geochim. Cosmochim. Acta* **58**, 1567–1579.

Sholkovitz E. R., Piepgras D. J. and Jacobsen S. B. (1989) The pore water chemistry of rare earth elements in Buzzards Bay sediments. *Geochim. Cosmochim. Acta* **53**, 2847–2856.

Sholkovitz E. R., Shaw T. J. and Schneider D. L. (1992) The geochemistry of rare earth elements in the seasonally anoxic water column and porewaters of Chesapeake Bay. *Geochim. Cosmochim. Acta* **56**, 3389–3402.

Siddall M., Khatiwala S., van de Flierdt T., Jones K., Goldstein S. L., Hemming S. and Anderson R. F. (2008) Towards explaining the Nd paradox using reversible scavenging in an ocean general circulation model. *Earth Planet. Sci. Lett.* **274**, 448–461.

Soyol-Erdene T.-O. and Huh Y. (2013) Rare earth element cycling in the pore waters of the Bering Sea Slope (IODP Exp. 323). *Chem. Geol.* **358**, 75–89.

Steiger R. H. and Jäger E. (1977) Subcommission on geochronology: convention on the use of decay constants in geo- and cosmochronology. *Earth Planet. Sci. Lett.* **36**, 359–362.

Stone A. T. and Morgan J. J. (1987) Reductive dissolution of metal oxides. In *Aquatic Surface Chemistry: Chemical Processes at the Particle–Water Interface*. John Wiley and Sons, New York, pp. 221–254.

Tachikawa K., Athias V. and Jeandel C. (2003) Neodymium budget in the modern ocean and paleo-oceanographic implications. *J. Geophys. Res. Oceans* **108**, 3254.

Tachikawa K., Toyofuku T., Basile-Doelsch I. and Delhaye T. (2013) Microscale neodymium distribution in sedimentary planktonic foraminiferal tests and associated mineral phases. *Geochim. Cosmochim. Acta* **100**, 11–23.

Tachikawa K., Piotrowski A. M. and Bayon G. (2014) Neodymium associated with foraminiferal carbonate as a recorder of seawater isotopic signatures. *Quat. Sci. Rev.* **88**, 1–13.

Takahashi Y., Hayasaka Y., Morita K., Kashiwabara T., Nakada R., Marcus M. A., Kato K., Tanaka K. and Shimizu H. (2015) Transfer of rare earth elements (REE) from manganese oxides to phosphates during early diagenesis in pelagic sediments inferred from REE patterns, X-ray absorption spectroscopy, and chemical leaching method. *Geochem. J.* **49**, 653–674.

Takebe M. (2005) Carriers of rare earth elements in Pacific deep-sea sediments. *J. Geol.* **113**, 201–215.

Toyoda K. and Tokonami M. (1990) Diffusion of rare-earth elements in fish teeth from deep-sea sediments. *Nature* **345**, 607–609.

Turner S., Sandiford M., Reagan M., Hawkesworth C. and Hildreth W. (2010) Origins of large-volume, compositionally zoned volcanic eruptions: new constraints from U-series isotopes and numerical thermal modeling for the 1912 Katmai-Novarupta eruption. *J. Geophys. Res. Solid Earth* **115**, B12201.

Vance D., Scrivner A. E., Beney P., Staubwasser M., Henderson G. M. and Slowey N. C. (2004) The use of foraminifera as a record of the past neodymium isotope composition of seawater. *Paleoceanography* **19**, PA2009.

van der Zee C., Roberts D. R., Rancourt D. G. and Slomp C. P. (2003) Nanogoethite is the dominant reactive oxyhydroxide phase in lake and marine sediments. *Geology* **31**, 993–996.

Walinsky S. E., Prahl F. G., Mix A. C., Finney B. P., Jaeger J. M. and Rosen G. P. (2009) Distribution and composition of organic matter in surface sediments of coastal Southeast Alaska. *Cont. Shelf Res.* **29**, 1565–1579.

White W. M. (2013) *Geochemistry*. Wiley-Blackwell.

White A. F. and Brantley S. L. (2003) The effect of time on the weathering of silicate minerals: why do weathering rates differ in the laboratory and field? *Chem. Geol.* **202**, 479–506.

Wilson D. J., Piotrowski A. M., Galy A. and McCave I. N. (2012) A boundary exchange influence on deglacial neodymium isotope records from the deep western Indian Ocean. *Earth Planet. Sci. Lett.* **341–344**, 35–47.

Wilson D. J., Piotrowski A. M., Galy A. and Clegg J. A. (2013) Reactivity of neodymium carriers in deep sea sediments: Implications for boundary exchange and paleoceanography. *Geochim. Cosmochim. Acta* **109**, 197–221.

Wolff-Boenisch D., Gislason S. R., Oelkers E. H. and Putnis C. V. (2004) The dissolution rates of natural glasses as a function of their composition at pH 4 and 10.6, and temperatures from 25 to 74 °C. *Geochim. Cosmochim. Acta* **68**, 4843–4858.

Wu Q., Colin C., Liu Z., Thil F., Dubois-Dauphin Q., Frank N., Tachikawa K., Bordier L. and Douville E. (2015) Neodymium isotopic composition in foraminifera and authigenic phases of the South China Sea sediments: Implications for the hydrology of the North Pacific Ocean over the past 25 kyr. *Geochem. Geophys. Geosystems* **16**, 3883–3904.

Xiong Z., Li T., Algeo T., Chang F., Yin X. and Xu Z. (2012) Rare earth element geochemistry of laminated diatom mats from tropical West Pacific: Evidence for more reducing bottomwaters and higher primary productivity during the Last Glacial Maximum. *Chem. Geol.* **296–297**, 103–118.

Zinder B., Furrer G. and Stumm W. (1986) The coordination chemistry of weathering: II. Dissolution of Fe(III) oxides. *Geochim. Cosmochim. Acta* **50**, 1861–1869.

Associate editor: Tina van de Flierdt